POUR POINT REDUCTION OF HEAVY CRUDE OILS BY THERMAL TREATMENT

By

DIANA BRAY FENTON

Bachelor of Science

in Chemical Engineering

Oklahoma State University

Stillwater, Oklahoma

1983

Submitted to the Faculty of the Graduate College
of the Oklahoma State University
in partial fulfillment of the requirements
for the Degree of
MASTER OF SCIENCE
May, 1987

POUR POINT REDUCTION OF HEAVY CRUDE

OILS BY THERMAL TREATMENT

Thesis Approved:

Billy L. Crynes
Thesis Adviser

Gary L. Foutch

Mayis Seapan

Marmon N. Dunham
Dean of the Graduate College

PREFACE

I wish to express my sincere gratitude to all the people who assisted me in this work and during my stay at Oklahoma State University. In particular, I am grateful to my major adviser, Dr. Billy L. Crynes for his help.

I am also thankful to the rest of the faculty in the Chemical Engineering Department for making my education there a good experience.

Special thanks are in order to the School of Chemical Engineering for the financial support I received during the course of this work.

Finally, I must thank my mother and father and brothers Ron and Glenn and mostly my husband Jeff for their constant support, encouragement, and understanding without whose help this work would not have been possible.

TABLE OF CONTENTS

LIST OF TABLES

LIST OF FIGURES

Figure Page

CHAPTER I

INTRODUCTION

Because of the uncertain future of easily processed crude oil and the fluctuating price of oil, interest in heavy crudes such as oil obtained from shale and tar sands continue to grow. Heavy crudes can be compared to average crudes as oils with higher viscosity, higher sulfur, metal and asphaltene contents, higher average boiling points, low hydrogen/carbon ratios, and higher pour points (1). These crudes contain large amounts of wax (high boiling straight chain paraffinic hydrocarbons) which impart to the crudes high pour points and cause the crudes to exhibit non-Newtonian viscosities. A minimum of upgrading is required for these oils to be transportable by pipeline.

The visbreaking process is currently undergoing a revival because it is a mild cracking process intended to reduce the viscosity and pour point of heavy petroleum fractions. In visbreaking, the viscosity of a crude is reduced by thermal cracking to a reaction product of lower molecular weight, lower boiling range, higher API gravity, and lower pour point than the original crude (2). As shown in the next chapter, little information is available in the literature on reactor parameters as they influence pour point.

An experimental apparatus was modified utilizing an unpacked, downflow reactor to study the effect of temperature and space time on the pour point of two whole crudes. The experiments were conducted at

atmospheric pressure and at temperatures of 400, 500 and 600°C (752, 932 and 1112°F). The flow rate of the crudes varied corresponding to a space time of 0.4 to 15 seconds. The reactor was made of 304 stainless steel. The product gas components were analyzed by gas chromatography and the liquid products were analyzed for a carbon/hydrogen weight ratio. Carbon deposited on the reactor walls was determined by a burning-adsorption method.

CHAPTER II

LITERATURE SURVEY

The process known as thermal cracking has historically been used to reduce the viscosity and pour point of heavy crudes and increase the amount of lighter distillates (those boiling below 350°C (662°F)). This process had its origin in a 1911 patent issued to Jesse Dubbs where the first continuous thermal cracking was described (3). In 1915, UOP Inc. was formed for the purpose of developing this Dubbs patent and in 1919 a semi-commercial thermal plant was demonstrated (4). This thermal cracker was a low capacity, single heating coil unit which fed whole crude to a separator where gases were produced. The reduced crude from the separator was then recycled to a heater which warmed the incoming crude before it was sent to a reaction chamber. In the reactor, or visbreaker, more gases were produced and the residual oil was sent to storage. The product gases entered the separator, and then the total gases from the separator were sent to a distillation column where fuel gas and distillate were made.

As mentioned, these reactors were low capacity, but by 1928 they had grown, run times increased, and single coil units became double coil units. The yields of desirable gasoline and light distillates increased if the crude charge was processed to coke instead of residuum. Coke is the carbonaceous deposit formed during visbreaking; whereas, residuum is the very heavy material (fluid) left from cracking (boiling above 565°C

(1049°F)) (5). In fact, many refiners ran their reactors as cokers by closing the valve that sent the residuum to storage. Eventually, the reactor filled with coke and the process was shutdown, the reactor was emptied and the process restarted. Next, a second reactor or coke chamber was added and the process then became a semi-continuous operation.

In the early 1940's, fluid catalytic cracking processes began and thermal cracking and coking declined. Catalytically cracked gasoline had several improved properties over thermally cracked gasoline; hence, thermal crackers and cokers were shutdown. Fluid catalytic cracked gasoline had higher octane and was more easily stabilized than thermally cracked gasoline (6). Since the market for catalytically cracked residuals was poor, the first delayed or low pressure cokers appeared in the early 1950's. They produced gas oil feed for the catalytic cracker from these unmarketable residuals. Low pressure coking is an operation to upgrade the highest boiling material in the crude. If the refinery did not have a delayed coker facility, these residuals were sold as fuel oil. However, the residuals could only be sold in this market after the addition of a distillate diluent stream (cutter stock) which reduced the fuel oil viscosity and pour point. Since residual fuel oil was a low price product, refiners tried to minimize its production. This was accomplished by what became known as visbreaking. Visbreaking reduced the production of fuel oil by approximately 20 percent. About 10 percent of the reduction could be accounted for by conversion to gas and gasoline while the reduction in viscosity and pour point decreased the cutter stock requirement by 10 percent (4).

There are two basic types of visbreakers. The first is a thermal gas oil unit named for the product usually desired, gas oil. The feed is the fraction of the crude with a boiling point above 350°C (662°F). In a thermal unit, the feed is cracked in the first furnace and goes to a fractionator. A side stream heavier than gas oil, the 350-450°C (662-842°F) fraction, is recovered from the fractionator and cracked again under more severe conditions in a second furnace. The effluent from this furnace is recycled to the fractionator. In the second type of visbreaker, the feed is the fraction of the crude boiling above 550°C (1022°F). The process is described in detail later in this report. The products from the two operations are similar. However, the first thermal cracking process offers better stability of the cracked residue and final fuels after blending with a diluent stream (6).

As the demand for petroleum products increased during the 1960's and 1970's, the reserves of easily processed conventional crude oils were depleted, and reliance upon poorer quality crude feedstocks grew. These poorer quality crudes which had previously been shunned often were of high wax content resulting in a high pour point, both of which made them difficult to refine and transport. In an article by Yepsen and Jenkins (8), a forecast of crude feedstocks based on quantity and quality of known reserves was published. It states that crude quality is constantly deteriorating. From 1976 to the year 2000 the average sulfur content of refinery charge is predicted to increase from 0.83 weight percent to 1.12 weight percent, and the API gravity will decrease from 34.8° to 31.4°. Because a minimum of upgrading of these waxy crudes is required to produce an oil that is transportable by pipeline,

interest in the visbreaking process revived as a way to use these less desirable feedstocks.

The ease of the visbreaking process has resulted in recent renewed interest in visbreaking (9, 10, 11). The factors that make visbreaking attractive are its relatively simple and rugged technology and readily available process equipment can be used. In fact, Shell Oil (12) in 1981 had twenty thermal crackers/visbreakers in operation, with 15 licensed visbreaking units in development. Also, as of 1983, there were 10 visbreakers and two thermal crackers in operation within Exxon (11).

Current visbreakers have two major vessels, a fired heater and a fractionator either with or without a soaking drum. The visbreaker feed is preheated by exchange with the product streams before it enters the heater coil where conversion occurs. In some instances, an unheated soaking drum is used in conjunction with a single zone heater. The soaking drum serves to replace the soaker zone but provides a longer residence time, thereby allowing heater operation at a lower effluent temperature which results in lower fuel consumption. The time-temperature trade off (high temperature - low space time as in the coil unit; low temperature - high space time as in the soaker unit) is claimed to have no significant effect on the kinetics, yields, and product qualities at a given equivalent operating severity (8).

The two current commercial visbreaking processes are the coil or furnace type visbreaker and the soaker visbreaker. Since visbreaking involves only a thermal reaction, the main operating variables are temperature and reaction time. Coil visbreaking may be described as a high temperature, short residence time process while soaker cracking

uses a low temperature, long residence time process. Yields of both processes are essentially the same as are the properties of the products. However, with the soaker process, fuel consumption is approximately 30 percent lower and investment cost is approximately 15 percent lower (13). The only difference between the two processes is that the soaker places all extra vessel between the furnace and the fractionator to increase the residence time and lower the temperature.

Little is published about the effect of visbreaking on the pour point of whole crudes. One of the first references to reducing the pour point by visbreaking occurred in 1950 where a high pour point waxy vacuum tower sidestream was visbroken with a 22-28°C (40-50°F) drop in pour point recorded (14). Heavy crudes with 12-15°API gravities and pour points of 21-38°C (70-100°F) were also visbroken to yield products with pour points of -6.7 - -3.9°C (20 - 25°F). No operating conditions were mentioned, however. The combination process of visbreaking plus gas oil cracking for pour point reduction was developed in the early 1960's primarily for North African waxy crudes. Few other references mention the effect of visbreaking on pour points until the late 1960's. In 1969, Nelson stated that pour point reductions of 11-17°C (20-30°F) were possible by visbreaking (15). Much later, in 1978, the only operating parameters associated with the reduction of pour point in the visbreaking process were discussed. Cracking temperatures of 480 to 500°C (896 to 932°F) and a furnace outlet pressure of two bars (1.97 atm) yielded a 6°C (10.8°F) reduction of pour point (7). Then, in 1979, Rhoe and de Blignieres displayed a relationship between pour point improvement and cracking severity (16). This showed that pour point reduction was proportional to the severity of visbreaking. However,

once again, no details of operating parameters were discussed, thus, in 1981, discussed the revival of visbreaking and cited visbreaking as useful in reducing the pour point of fuel oil from waxy feedstocks, such as those originating from Libyan crudes. Reductions of 15-20°C (27-36°F) were mentioned (17).

The exact mechanism by which the crude pour point is reduced during visbreaking is not completely understood (18). There are broad classes of crude oil compounds: hydrocarbons, resins, and asphaltenes. Asphaltenes are high molecular weight agglomerates held together by physical forces. Resins are considered very high molecular weight compounds which can be separated from a deasphalted residue by absorption. The hydrocarbons act as the continuous phase. During visbreaking, two general processes are believed to take place. The continuous hydrocarbon phase is cracked to form smaller molecules. The paraffins are mostly cracked to smaller paraffins and olefins. Practically no carbon and hydrocarbon are formed (at least not by design) so that no coke formation takes place in the primary cracking. Some olefins may crack to form either two smaller olefins or an olefin and a diene. The dienes are usually of short chain length and are more likely formed at higher temperatures. The asphaltenes are held in a stable colloidal solution or remain in suspension up to a certain degree of conversion. Past this conversion, if the cracking is too severe, the colloidal solution cannot be maintained and the asphaltenes separate, form deposits or sludge, and are unstable. This instability sets the upper conversion limit of a typical visbreaking process (16, 17). The second reaction process is coke formation which occurs through

polymerization, condensation, dehydration, and dealkylation reactions (19).

Coke formation governs the length of time a visbreaker may be operated. Coking rates are generally a function of temperature and fouling tendency of the product. As the cracking severity increases, more and more coke is laid down on the reactor walls. Coking rates are considerably higher in coil units than in soaker units (12).

The problems associated with handling and transporting waxy, high pour point crude oils are many. During winter, crystallization of straight chain paraffins causes the entire mass of oil to gel near its pour point temperature. This makes pipeline transport a tricky problem. This means that the temperature of the crude must be maintained above its pour point to permit handling. Therefore, transportation costs tend to be high because of the special pumping and heating requirements. Additionally, waxy components are deposited on pipeline walls and must be occasionally removed. If a pipeline pump failure occurs, the crude could cool to a temperature below its pour point, resulting in a solid mass of oil in the pipeline. Restarting such a pipeline is difficult.

Thermal treatments are well known as means to improve the transportability of problem crudes. In 1971, British Petroleum and the Burmah Oil Company published a scheme by which 29°C (85°F) pour point Assam (India) crude could be pumped at 18°C (65°F). Their scheme involves first heating the crude to 95°C (203°F) and then cooling it to 65°C (149°F) under carefully controlled shearing action. Further cooling to 18°C (65°F) is then accomplished by allowing the crude to cool statically at a predetermined rate (0.3-1.4°C/min (0.5-

2.5°F/min)). Because of considerable success using this process, two large scale plants have been built. The alternatives to the heat treatment process are:

1. emulsification with water and surfactants
2. use of a water layer between the crude and pipewall
3. dilution with a solvent or low pour point crude
4. heating the crude prior to transport so that it never cools to near its pour point
5. addition of pour point depressants

All these methods have their advantages and disadvantages (20, 21, 22).

One of the most popular methods of reducing the pour points of whole crudes is by additives known as pour point depressants. These additives are dissolved in the crude oils at concentrations usually less than one percent. They are typically copolymers of ethylene and vinyl acrylates. These compounds reduce the pour point by interfering with the crystal structure of the wax as the crude cools to its normal pour point. The pour point depressants, some believe, incorporate themselves into the wax crystals during precipitation. The depressants lower the pour point by preventing the normal agglomeration of the wax crystals into a solid mass. Pour point reductions of approximately 20°C (36°F) have been reported (22, 23, 24).

Since very little about pour point reduction is known and since increased refining of poorer quality crudes is inevitable, continued research in the area of visbreaking is called for. Studies of the alternative methods of lowering pour points and the mechanisms by which they occur are necessary.

CHAPTER III

METHODS AND PROCEDURES

Apparatus

All experiments were conducted in an unpacked, downflow tubular reactor. The flow system is shown in Figure 1, and reactor details are shown in Figure 2. From the left side, nitrogen and oxygen were sent to the reactor. The gases passed through calibrated Matheson flowmeters in 0.64 cm (0.25 in) stainless steel tubing. The reactor was made of 304 stainless steel tubing and was 0.64 cm (0.25 in) outer diameter and 30.5 cm (12 in) long. An adjustable chromel-alumel thermocouple and thermowell were centered inside the reactor tube. The thermowell consisted of 0.32 cm (0.12 in) stainless steel tubing. The exact dimensions of the reactor with the thermowell were 0.24 cm (0.094 in) annular space, 30.5 cm (12 in) long. The reactor was placed inside a copper block which was electrically heated by ceramic beaded resistance wires. The temperature profile in the reactor was maintained by a Hewlett Packard Temperature Controller 240. After the preheat zone when the temperature stabilized, the average temperature difference along the length of the reactor was 30°C (86°F). The crude oil was fed into the preheat zone by a Harvard Syringe Infusion/Withdrawal Pump using 2.0 ml syringes through 0.64 cm (0.25 in) outer diameter flexible rubber tubing. In the preheat zone, the oil was pumped through 0.32 cm (0.125 in) outer diameter, 304 stainless steel tubing; to the reactor. The

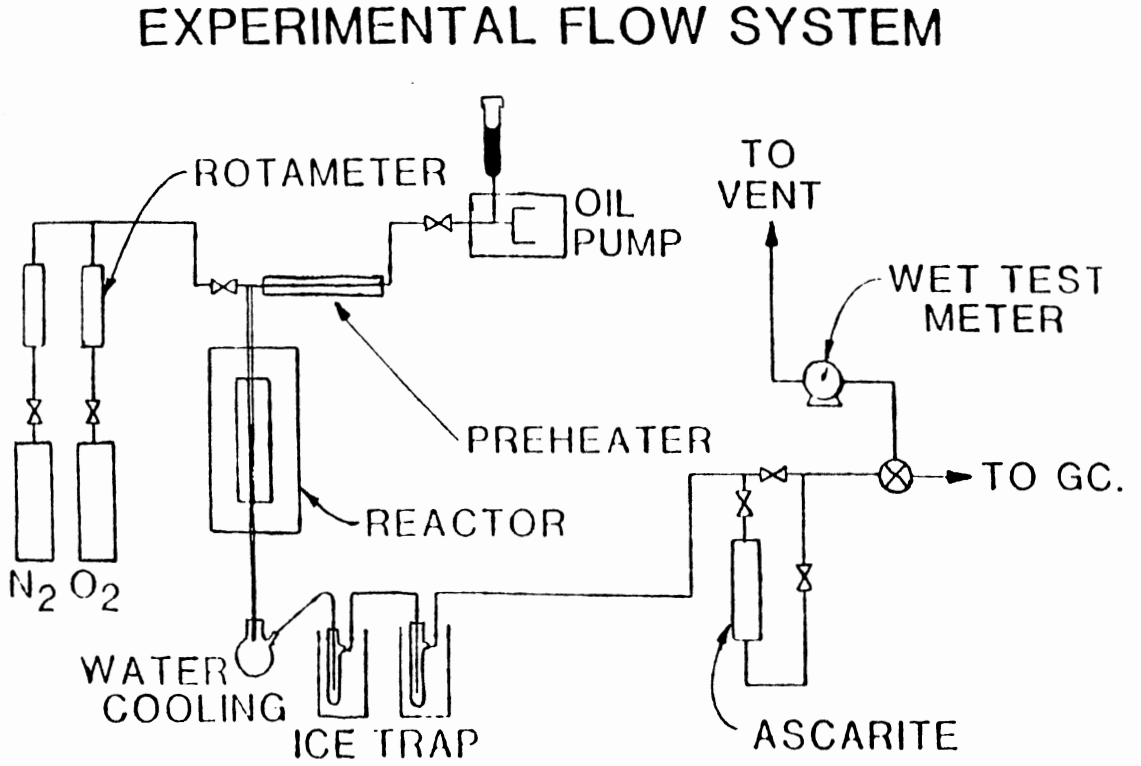

Figure 1. Experimental Flow System

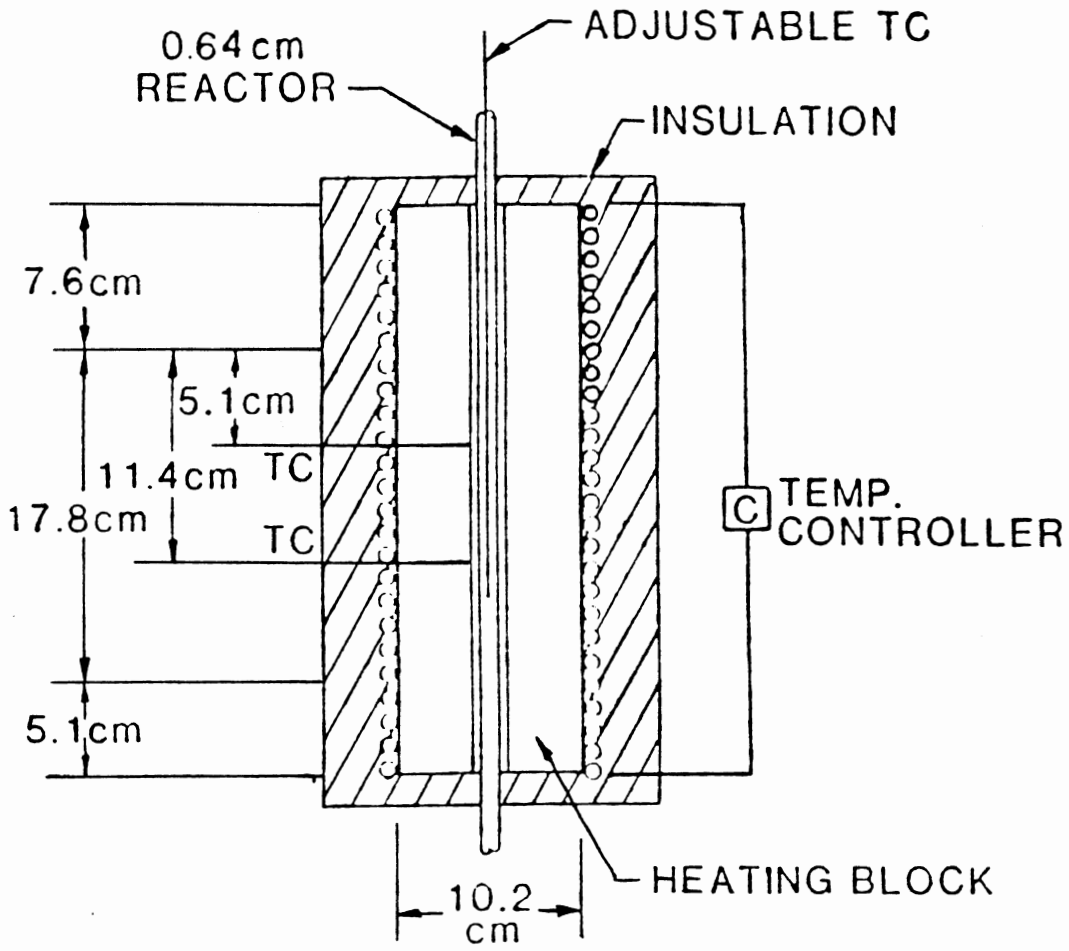

Figure 2. Reactor Details

unvaporized crude oil then flowed down the sides of the reactor into a water cooled 250 ml Erlenmeyer receiving flask. The vaporized product traveled from the cooled flask through 0.64 cm (0.25 in) heavy rubber tubing to a series of cold traps. The cold traps (ice) were connected by 0.64 cm (0.25 in) Tygon tubing and then connected to 0.64 cm (0.25 in) copper tubing where the gases passed to a sample port, Ascarite II drying tube, and wet test meter in series. The wet test meter was connected to a vent hood by 1.59 cm (0.625 in) Tygon tubing. The total gas volume was measured by a calibrated wet test meter. All thermocouples (reactor, preheat and heat block) were calibrated at low temperatures (0-350°C (32-662°F)) by a Rosemount Model 910 variable temperature oil bath, and at high temperatures (350-650°C (662-1202°F)) by a Thermocouple Checking Furnace from Leeds and Northrup.

All condensables carried along with the gas stream were separated by the series of traps. The gas components were then analyzed by a Hewlett Packard 5890 gas chromatograph (GC) equipped with a flame ionization detector. Carbon that formed in the reactor was burned with oxygen to yield carbon dioxide, which was adsorbed on the Ascarite II.

The model numbers of all equipment and chemicals used in this study are listed in Appendix A.

Quantitative Analysis

The major components in the gaseous fraction from pyrolysis (visbreaking) of the crudes were hydrogen, light alkanes, and light alkenes. The concentration of each component, except hydrogen, was determined by simple area ratios from the chromatograms. This method was used over the response factor method since all components were light

gases and their response factors were found to be close to 1.00. More detail on the response factor method is given in Appendix B. Hydrogen formation was not analyzed in this study due to analytical limitations. The chromatograph was calibrated using standards to identify individual component retention times. These standards are given in Appendix A.

Feedstocks

Two feedstocks were used; both supplied by Conoco, Inc., Ponca City, Oklahoma. One originated from Ikan Pari in Indonesia and had a pour point of 27°C (80°F) as measured by ASTM D97. The other crude was from the Udang Sea in the People's Republic of China and had a pour point of 40°C (105°F). These crudes were chosen because of their relatively high values and range of pour points. The properties of the feedstocks are given in Table I.

Operating Procedures

The experiments were conducted at atmospheric pressure at temperatures of 400, 500 and 600°C (752, 932 and 1112°F). The crude oil flow rate varied from 0.79 to 3.93 ml/min which corresponds to a space time (discussed in detail in discussion chapter) of 0.4 to 15 s.

The temperatures of the reactor and preheat zone were allowed to reach steady state for at least 4.0 h before each experimental run. The GC was allowed to reach steady state for at least 1.0 h before each experimental run. Nitrogen was passed through the reactor system at 500 ml/min for 1.0 h before the run was started to purge oxygen. After the reactor had reached the desired temperature, the oil was pumped through

TABLE I

FEEDSTOCK PROPERTIES

Distillation - ASTM D1160 (Converted to atmospheric pressure)	Crude A	Crude B
Vol. %	T (°F)	T (°F)
5	549	784
10	630	874
15	705	918
20	779	1081
30	838	1231
40	1000	1333
50	1099	1499 (endpoint)
60	1216	
70	1339 (endpoint)	
Density (g/ml)	0.79	0.83
API gravity - ASTM D287	48°	37°
Viscosity - ASTM D445 (cp)	at 80°F, 2.38 90°F, 2.12 100°F, 1.95	130°F, 8.71 150°F, 6.20 180°F, 3.97
Sulfur content - ASTM D1552 (wt%)	0.02	0.05
Pour Point - ASTM D97	80	105
Conradson Carbon (wt%)	0.5	3.0
C_H weight ratio	6.1	6.0

the preheater and into the reactor. Heat lamps were placed to warm the pump syringes and lines for the higher pour point crude to prevent solidification in the pump lines. The temperatures at each point, preheat and reactor, were controlled to within 4°C (7.2°F) during the experiment. The temperatures of the preheater wall and tube center were also monitored. These revealed a typical temperature difference of 5°C (9°F). The temperature variations along the length of the reactor were monitored and nominally differed by a maximum of 30°C (86°F).

The first gas sample was taken and injected into the GC 5 min after the run started. Subsequent sampling was done at approximately 10 min intervals. The GC signals were integrated and recorded by an HP integrator. The last sample was taken after 60 to 90 min. The liquid product collected in the receiver was later analyzed for a carbon-hydrogen weight ratio by a Perkin Elmer Elemental Analyzer.

Typical experimental runs lasted 60 to 90 min when enough liquid sample was collected. After the run was terminated, the liquid receiver was disconnected for further analysis. Nitrogen was flushed through the reactor at 600 ml/min for 30 min to sweep out residual gases before the decoking step started.

The carbon that formed during the experimental run was determined by passing a mixture of oxygen and nitrogen through the reactor at 500°C (932°F) and collecting the resultant carbon dioxide on Ascarite II. During coke removal, the nitrogen rich stream at start (from 400 ml/min N_2 to 200 ml/min N_2) was slowly converted to an oxygen rich stream (from 200 ml/min O_2 to 400 ml/min O_2) to prevent uncontrolled combustion. Since decoking is an exothermic reaction the temperature of the reactor outlet was monitored closely and normally rose 50°C (90°F). When the

temperature equilibrated to its starting point, the decoking step was stopped. This process took from 45 to 90 min. Nitrogen was then allowed to flow at 400 ml/min through the system for 15 minutes to eliminate any residual carbon dioxide. The difference in weight of the Ascarite before and after decoking was taken as the weight of carbon dioxide formed. Before another run was started, the system was purged with nitrogen at 600 ml/min for at least 1.0 h.

Appendix C (Table XVI) gives the operating conditions of the GC.

A total of twenty-five experimental runs including duplicates were conducted on the two crudes.

CHAPTER IV

RESULTS

The reactions for this study were carried out at temperatures of 400, 500, and 600°C (752, 932, and 1112°F) and feed flow rates of 0.79, 1.6, and 3.9 ml/min. The flow rates correspond to a space time within the reactor of 0.15 to 14.3 s. All combinations of temperature and flow rate (space time) were examined. The two variables, temperature and space time, are the variables of interest in pyrolysis reactions according to articles by Notarbartolo, Mengazzo and Kuhn (10) and Stolfa (4).

The results obtained in this study included product oil pour point, coke and gas formed, and gas composition. The liquid product was analyzed 24.0 h after each experimental run for its pour point.

As each run progressed, the gas composition changed as a function of time. Figures 3 and 4 illustrate typical time behaviors of the compositions of methane and ethane for crude A at 600°C (1112°F) and 1.57 ml/min which corresponds to a space time of 0.79 s. The three sets of data points illustrate data for replicate experimental runs. Table II lists the average amounts of each gaseous component formed for the various conditions for crude A. Table III lists similar results for crude B.

For crude A, the amount of gas and coke produced as a function of space time at various temperatures is listed in Table IV and shown in

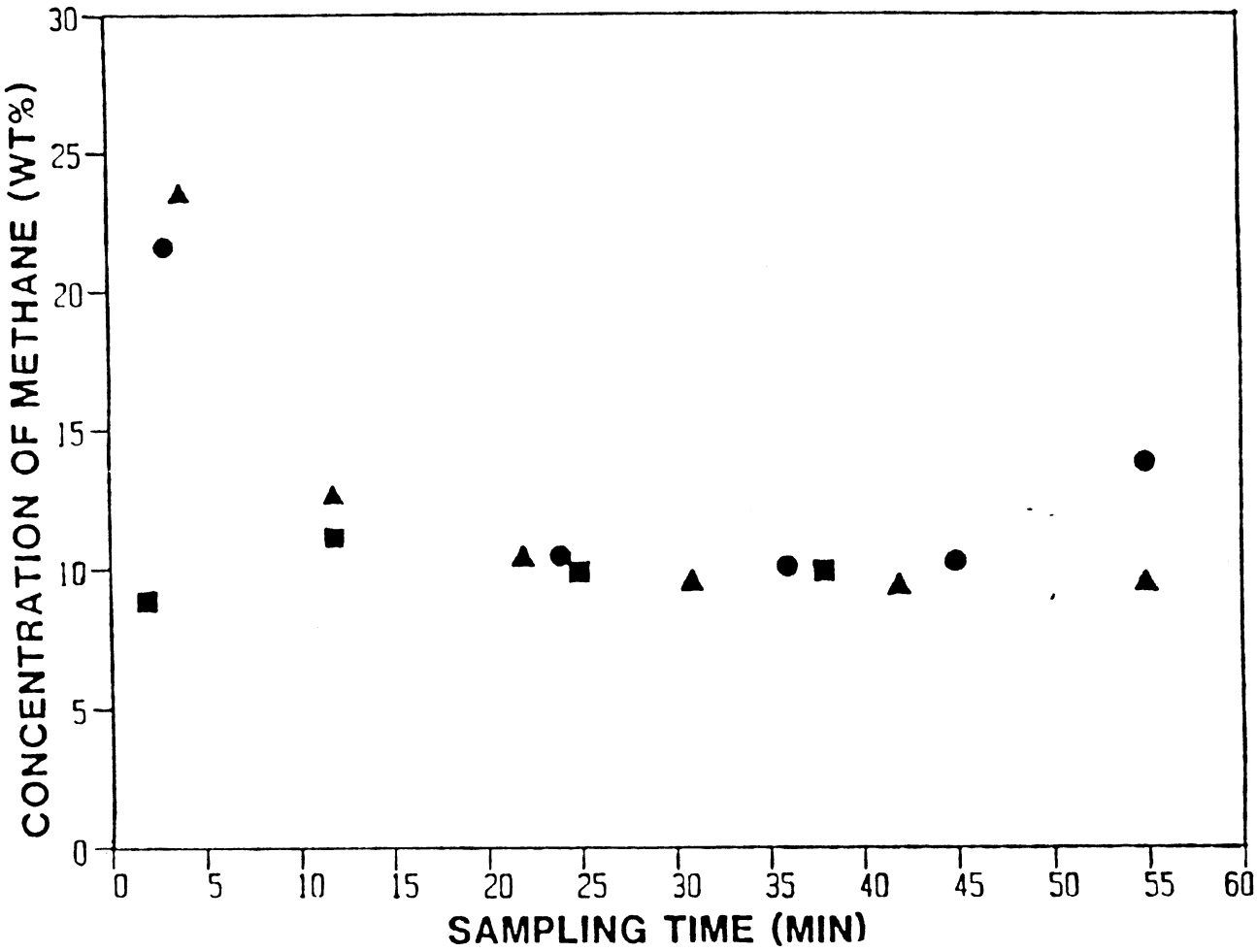

Figure 3. Concentration of Methane vs. Sampling Time - Crude A, 600°C
Symbols represent three identical experiments

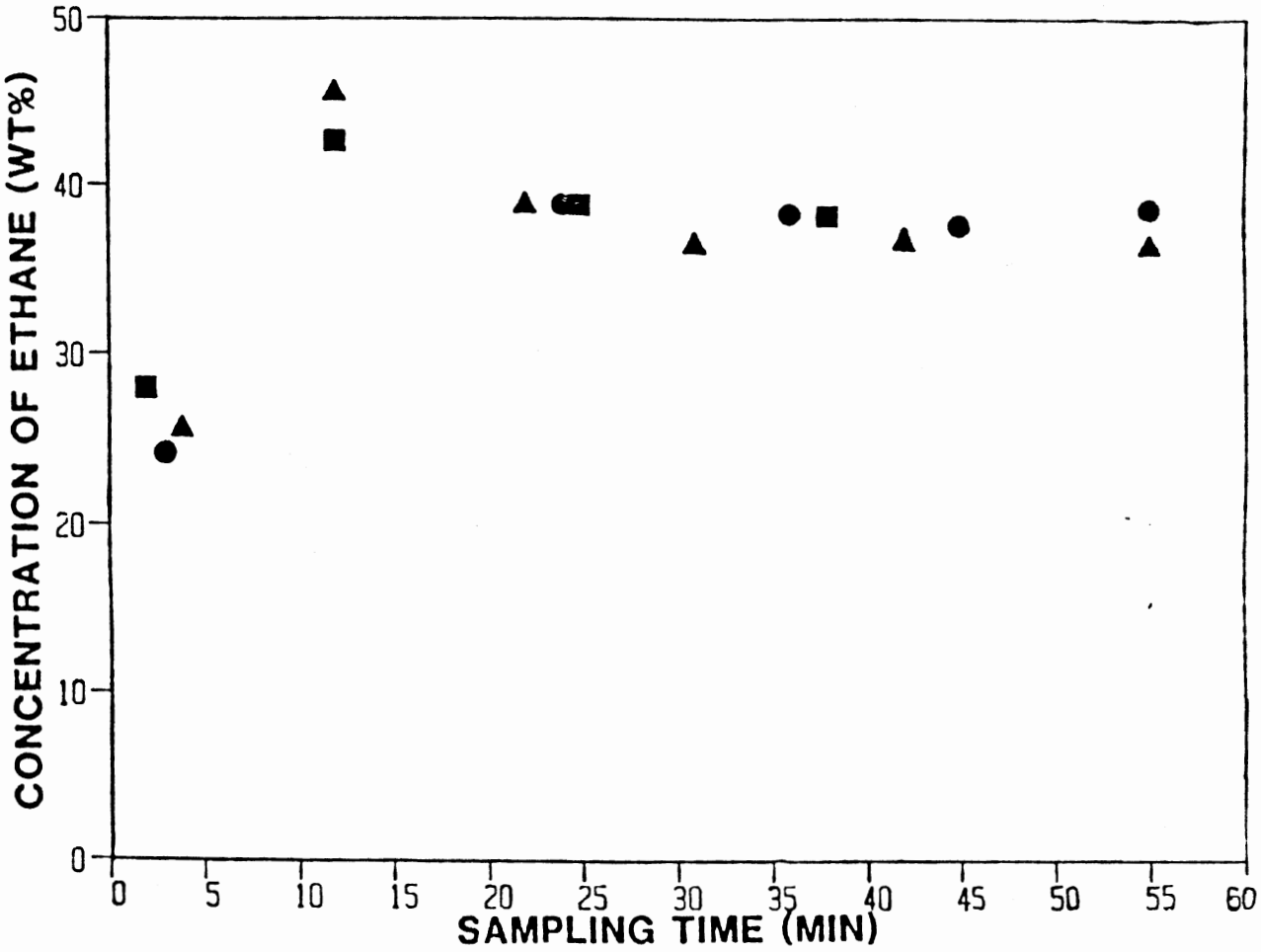

Figure 4. Concentration of Ethane vs. Sampling Time - Crude A, 600°C
Symbols represent three identical experiments

TABLE II

PRODUCT GAS COMPONENTS -
CRUDE A

Temp (°C)	400			500			600		
Flow Rate (ml/min)	3.9	1.6	0.8	3.9	1.6	0.8	3.9	1.6	0.8
Space Time (sec)	0.8	2.1	3.6	0.3	0.7	1.5	0.2	0.4	0.8
Run Number	13	34	19	9,38	36	17,21,42	11	40	24,44,46
Gas Made (wt%)(1)									
C_1	3.1	1.1	4.9	26.0	18.2	21.5	13.4	11.1	12.1
C_2's(2)	10.5	11.5	26.4	26.0	34.1	32.8	43.3	35.6	36.1
C_3's	19.5	21.0	34.5	24.0	23.4	20.8	24.3	26.0	26.7
C_4's	14.0	29.3	20.8	19.7	11.6	14.2	9.8	22.0	17.7
C_5's	33.3	37.2	14.5	7.6	10.4	8.8	5.1	6.2	8.1
C_6s	12.5	0	0	0	0	0.8	3.9	0	0

(1) wt% = wt. gas/total crude fed x 100
(2) alkanes, alkenes, alkynes

TABLE III

PRODUCT GAS COMPONENTS -
CRUDE B

Temp (°C)	400			500			600		
Flow Rate (ml/min)	3.9	1.6	0.8	3.9	1.6	0.8	3.9	1.6	0.8
Space Time (sec)	3.1	7.3	14.3	0.8	1.5	5.5	0.5	1.1	2.6
Run Number	48	56,58	57	49	52,59	60	55	54	61
Gas Made (wt%)(1)									
C_1	2.2	1.3	1.2	14.3	14.6	5.8	7.0	7.0	9.9
C_2's(2)	4.2	1.3	1.7	7.8	20.2	11.5	23.6	23.7	26.5
C_3's	12.9	4.1	7.5	14.1	22.0	5.3	13.1	14.1	20.6
C_4's	40.7	14.3	5.1	16.4	28.3	1.2	6.1	9.3	16.0
C_5's	29.4	38.4	12.5	47.3	17.0	0.4	0	5.3	10.0
C_6s	0	42.2	74.7	0	17.3	76.0	50.2	40.4	16.1

(1) wt% = wt. gas/total crude fed x 100
(2) alkanes, alkenes, alkynes

TABLE IV

PRODUCT FORMED: CRUDE A

Temp (°C)	400			500						600				
Flow Rate (ml/min)	3.9	1.6	0.8	3.9	3.9	1.6	0.8	0.8	0.8	3.9	1.6	0.8	0.8	0.8
Space Time (sec)	0.8	2.1	3.6	0.3	0.3	0.7	1.5	1.5	1.5	0.2	0.4	0.8	0.8	0.8
Run Number	13	34	19	9	38	36	17	21	42	11	40	24	44	46
Wt% Gas(1)	31	0.3	0.8	0.3-7	0.6-7	0.81	1.4	1.3	1.23	1.45	8.2	11.1	10.7	12.7
Wt% Coke(1)	.04	0.1	0.28	0.26	0.38	0.51	(2)	0.8	0.6	0.46	0.69	0.7	0.91	0.76
Pour Point (°F)	75	75	70	75	75	75	70	75	75	70	65	60	60	60
Liquid Product C/H (wt%)	6.25	5.89	6.01	5.91	5.94	6.02	6.05	5.93	5.82	6.13	5.92	6.15	6.26	6.27

(1) wt% = wt. gas (coke)/total crude fed x 100
(2) aborted rund

Figure 5 are the gas data. Figure 6 and Table V give the same data for crude B.

The amount of coke created as a function of space time and temperature is listed in Table IV and shown in Figure 7 for crude A. Likewise data for crude B are in Table V and Figure 8.

The curves drawn on all figures do not represent any regressed data. They are drawn to show trend only.

These data, both gas composition and carbon formation agree well with the little information available in the literature. According to Fujita et al., at a crude oil cracking temperature of 750°C and space time of 3.24 s, the product distribution of components analyzed (from C_1 to C_4 and coke) agree very well with the data collected here (25). Also, Wing (26) collected data (from C_1 to C_8) comparable to the data here. However, Wing states that furnace conditions are proprietary so that no direct comparison can be made. Apparently, judging from the literature, this type of experimental work is proprietary since little data have been published.

The effect of space time and temperature on pour points is listed in Table IV and shown in Figure 9 for crude A, and Table V and Figure 10 for crude B. A pour point reduction of 20°F was noted for both crudes. This agrees with Nelson (15) who reported that pour point reductions of 20-30°F were possible by visbreaking.

The length of time between liquid product formation and eventual pour point determination (sample gas) seemed to be a significant factor. Table VI presents this pour point-time effect. The lowest pour point was always measured immediately following thermal cracking. The

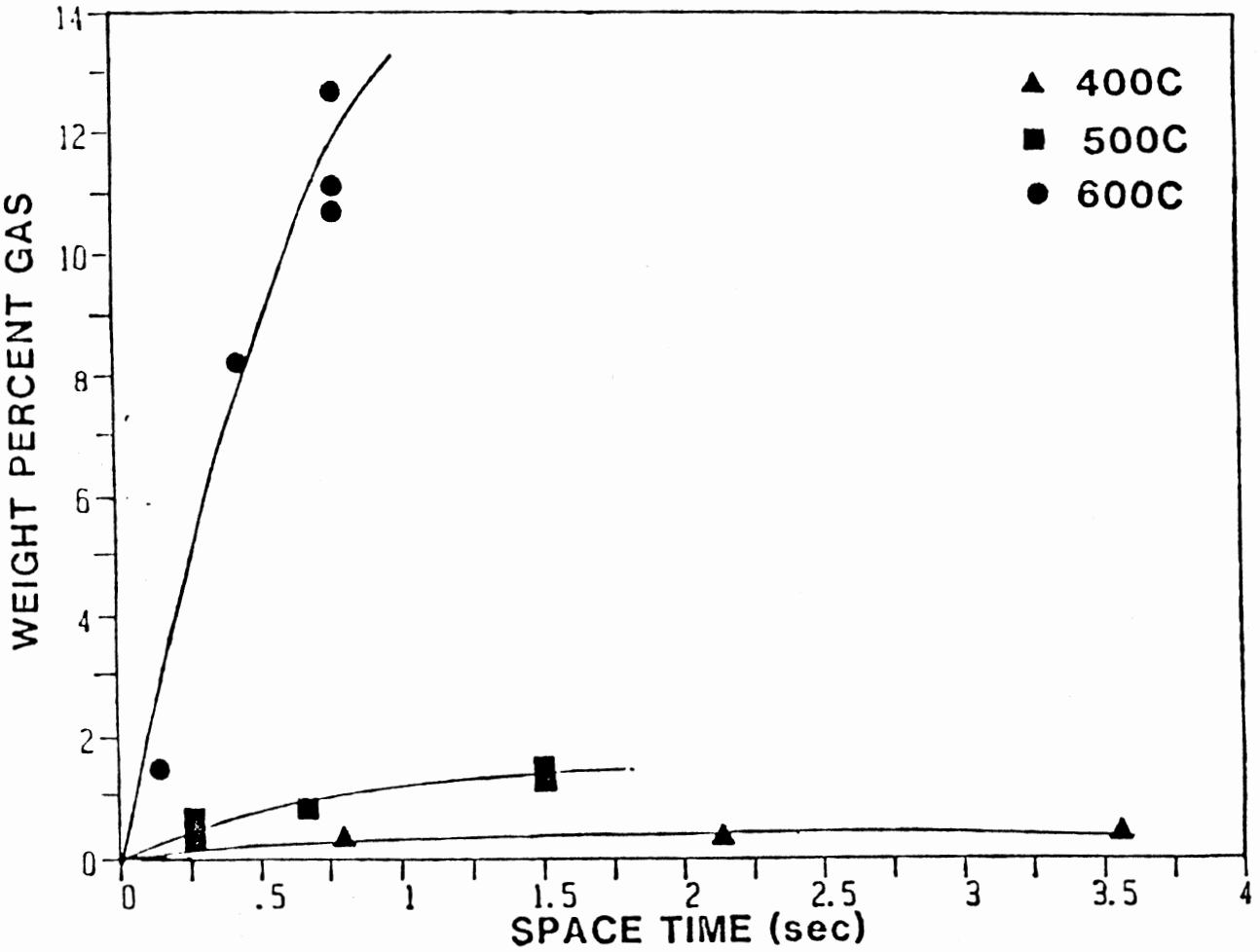

Figure 5. Weight Percent Gas Formed (of the feed) as a Function of Reactor Space Time - Crude A

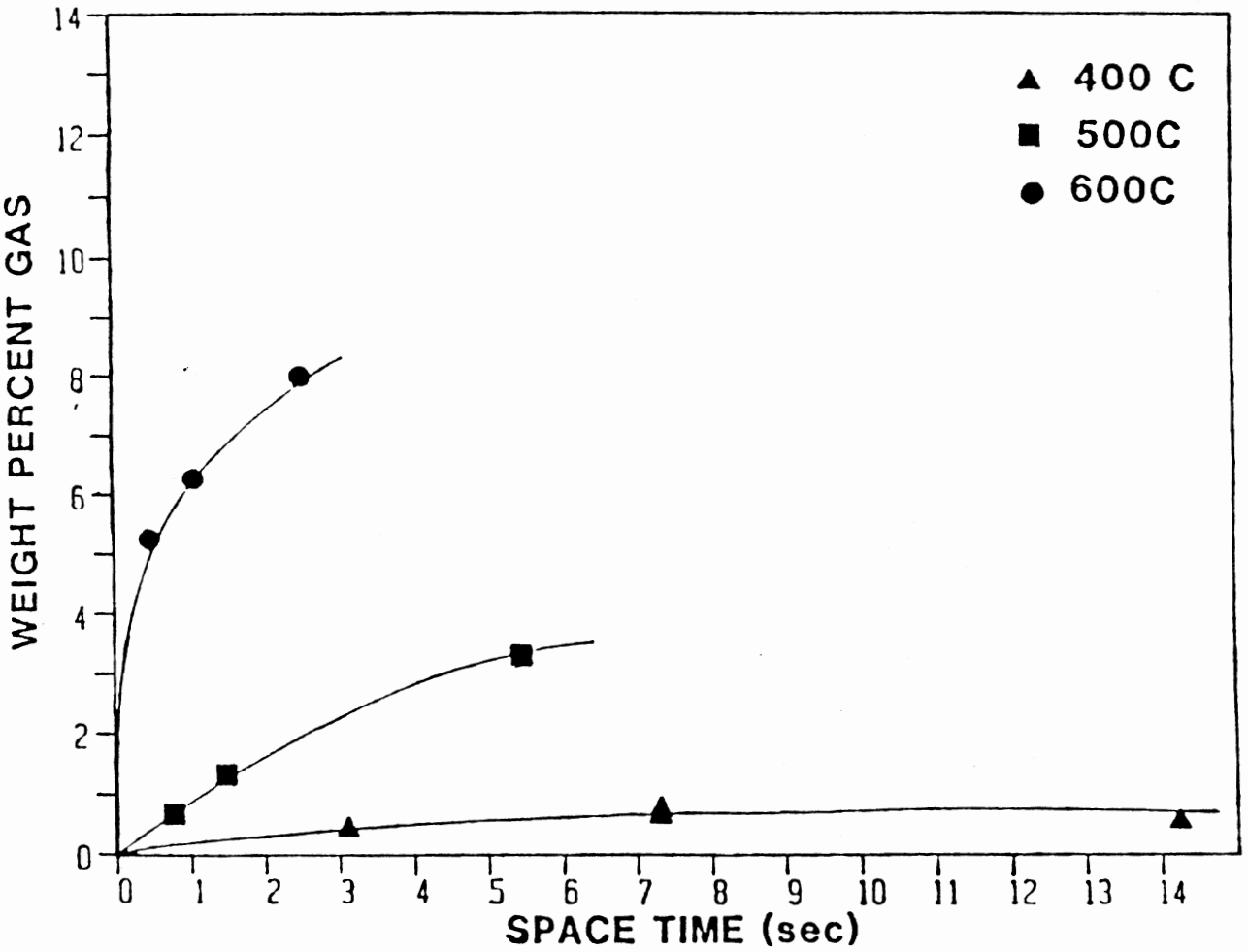

Figure 6. Weight Percent Gas Formed (of the Feed) as a Function of Reactor Space Time - Crude B

TABLE V

PRODUCT FORMED: CRUDE B

Temp (°C)	400				500				600		
Flow Rate (ml/min)	3.9	1.6	1.6	0.8	3.9	1.6	1.6	0.8	3.9	1.6	0.8
Space Time (sec)	3.13	7.8	.8	14.27	0.8	1.5	1.5	5.47	0.48	1.08	2.55
Run Number	48	56	58	59	49	50	59	60	55	54	61
Wt% Gas(1)	0.4	0.71	0.66	0.54	0.69	1.28	1.31	3.3	5.29	6.25	7.98
Wt% Coke(1)	0.05	0.12	0.18	0.11	0.44	(2)	1.88	2.1	2.0	2.38	2.4
Pour Point (°F)	105	105	105	105	100	100	100	100	95	90	85
Liquid Product C/H (wt%)	6.12	6.28	6.04	6.11	6.27	6.49	6.22	6.20	6.2	6.3	5.87

(1) wt% = wt. gas (coke)/total crude fed x 100
(2) aborted run

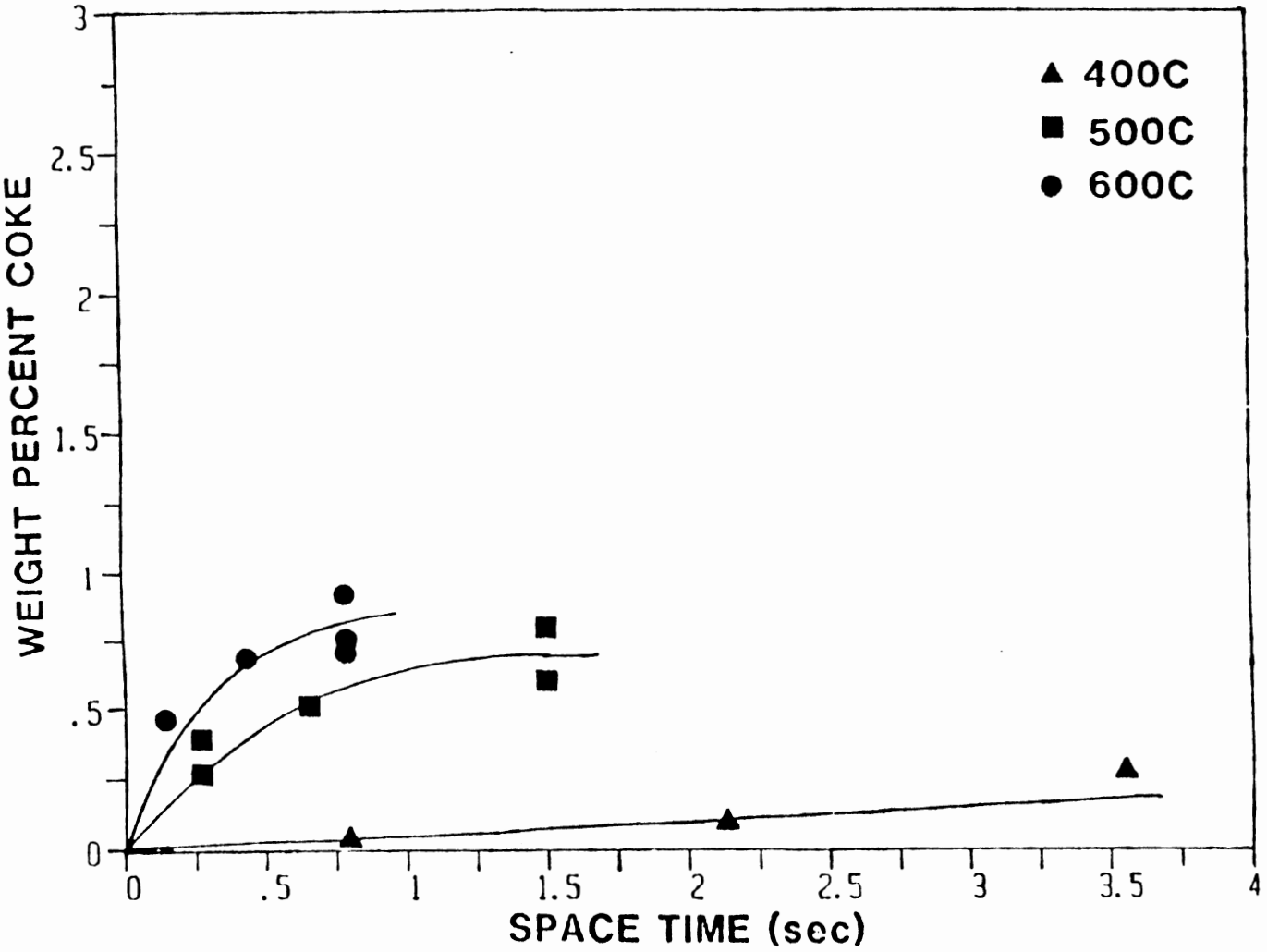

Figure 7. Weight Percent Coke Formed (of the Feed) as a Function of Reactor Space Time - Crude A

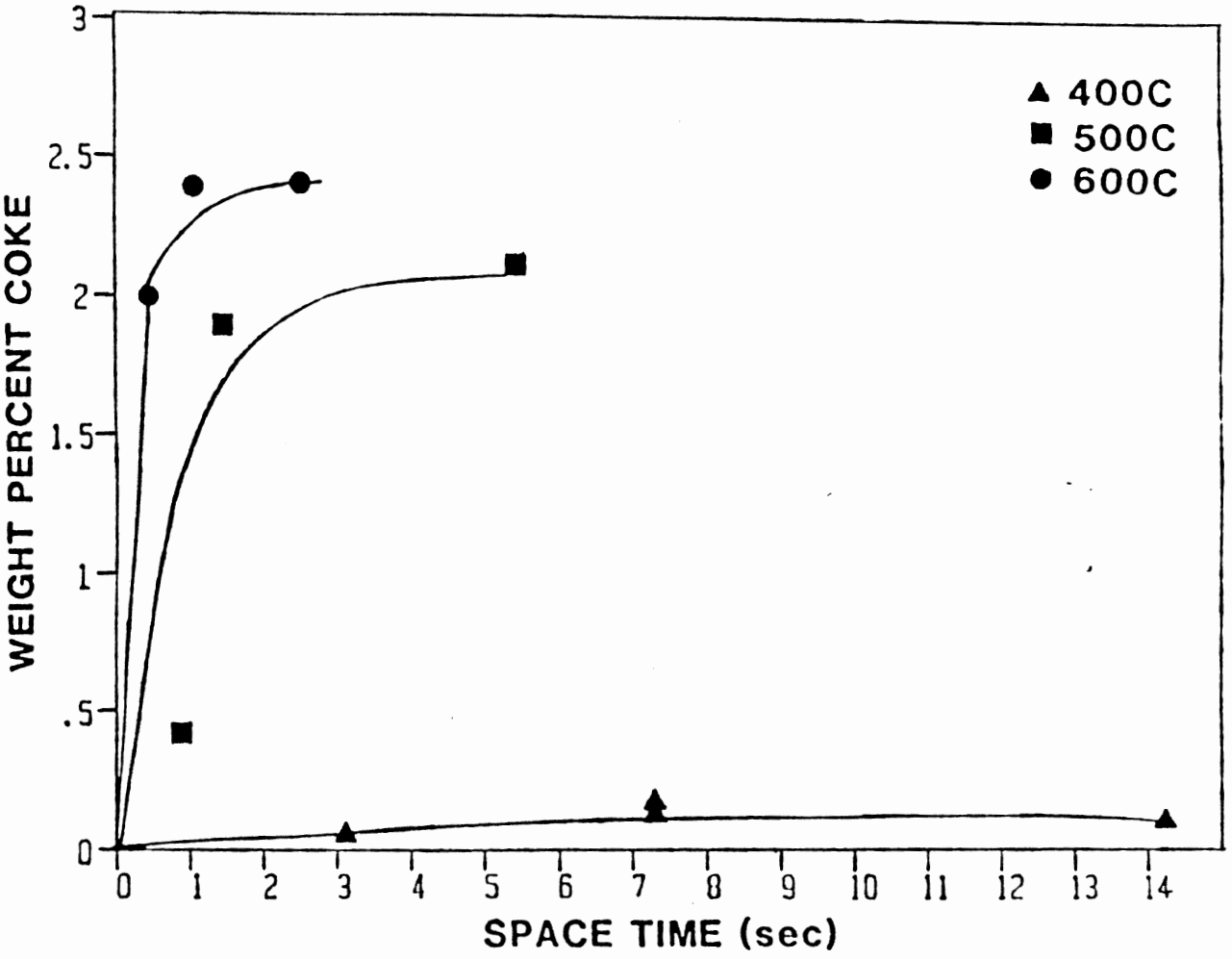

Figure 8. Weight Percent Coke Formed (of the Feed) as a Function of Reactor Space Time - Crude B

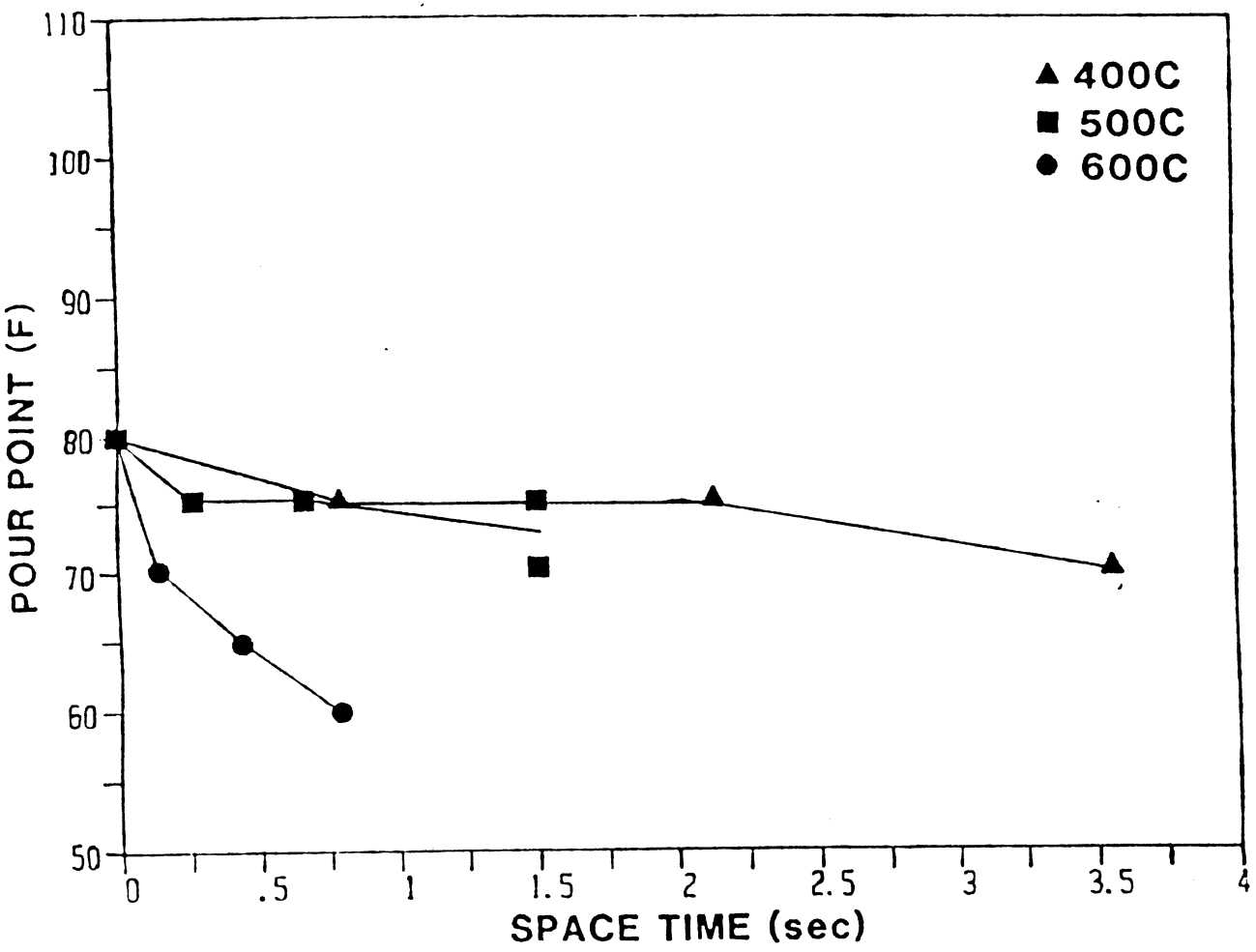

Figure 9. Pour Point as a Function of Reactor Space Time - Crude A

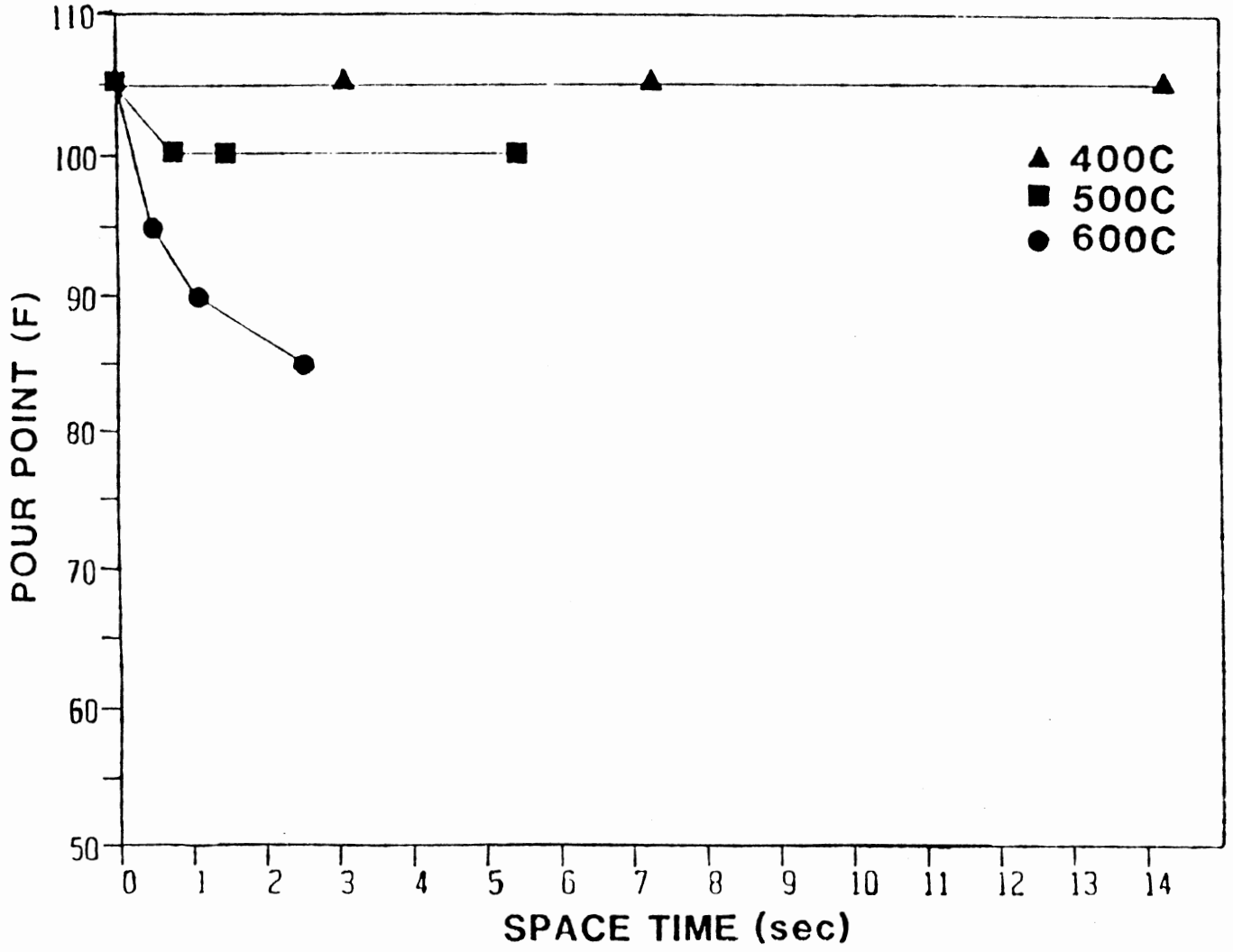

Figure 10. Pour Point as a Function of Reactor Space Time - Crude B

TABLE VI

POUR POINT AS A FUNCTION
OF SAMPLING TIME

Sampling Time (h)	Pour Point (°F)
1.2	60
19	65
43	65
73	65
120	65

pour point then increased 2.8°C (5°F) within 24 hr but remained constant thereafter.

Near the conclusion of this study, some preliminary data were obtained on the feedstocks and a few liquid product samples when a new GC system became available. The crudes, both before and after cracking, were analyzed by capillary gas chromatography on an HP 5880 equipped with a column 60 m x 0.32 mm, 1μ film thickness, DB-1 (methyl-silicone) and a thermal conductivity detector. Appendix C (Table XVII) gives the operating conditions of this GC. Table VII lists the retention times and area percents of the major peaks for untreated crude A; notice how all major peaks are paraffins. Table VIII lists the same for the visbroken liquid at conditions of 600°C (1112°F) and 0.79 ml/min which corresponds to a space time of 0.79 s. Table VIII shows that after visbreaking both paraffins and olefins appear in the sample. Table IX lists chromatographic details of untreated crude B (notice all major peaks are n-alkanes) and Table X lists those of the visbroken liquid (major peaks are now n-alkanes and α-olefins) and at conditions of 600°C (1112°F) and 0.79 ml/min which corresponds to a space time of 2.55 s. Figure 11 shows a typical chromatogram of the feedstock and visbroken liquid. The conversion of one peak to two peaks is easily seen. This chromatogram is for crude A, however, crude B showed an identical response. The fraction of the GC sample feed that was vaporized in the inlet system and, therefore, qualitatively determined is not known. However, for the components that the GC could elute; which were hydrogen, air, and hydrocarbons through C_{30}, there is a marked pattern of conversion of paraffins to paraffins and olefins.

Carbon/Hydrogen weight ratios were determined by a Perkin Elmer

TABLE VII

MAJOR COMPONENTS FOR 80°F
POUR CRUDE - UNTREATED

Component	Response Time (min)	Area Percent
nC_4	1.94	0.62
nC_5	2.85	0.14
nC_6	4.89	0.66
nC_7	9.25	1.80
nC_8	15.23	3.15
nC_9	21.61	3.91
nC_{10}	27.77	4.52
nC_{11}	33.55	4.93
nC_{12}	38.95	4.94
nC_{13}	44.01	4.95
nC_{14}	48.76	4.73
nC_{15}	53.24	4.32
nC_{16}	57.46	3.75
nC_{17}	61.46	3.15
nC_{18}	65.26	2.42
nC_{19}	68.88	2.10
nC_{20}	72.32	1.45
nC_{21}	75.62	1.08
nC_{22}	78.76	0.73
nC_{23}	81.78	0.56
nC_{24}	84.72	0.34
nC_{25}	88.08	0.25
Cn_{26}	92.09	0.15
nC_{27}	96.96	0.12
nC_{28}	102.89	0.07

TABLE VIII

MAJOR COMPONENTS FOR 80°F
VISBROKEN LIQUID

Component	Retention Time (min)	Area Percent
$nC_5^=$	2.73	1.62
nC_5	2.80	0.21
$nC_6^=$	4.57	4.09
C_6	4.76	0.05
$nC_7^=$	8.65	3.18
nC_7	9.26	0.64
$nC_8^=$	14.49	2.69
nC_8	15.22	1.15
$nC_9^=$	20.85	2.57
nC_9	21.58	1.63
$nC_{10}^=$	27.03	2.67
nC_{10}	27.73	2.31
$nC_{11}^=$	32.86	2.22
nC_{11}	33.51	2.99
$nC_{12}^=$	38.31	1.87
nC_{12}	38.92	3.82
$nC_{13}^=$	43.42	1.44
nC_{13}	43.98	4.34
$nC_{14}^=$	48.21	1.41
nC_{14}	48.73	4.28
$nC_{15}^=$	52.72	0.89
nC_{15}	53.20	3.74
$nC_{16}^=$	56.98	0.63
nC_{16}	57.42	2.85
$nC_{17}^=$	61.01	0.42
nC_{17}	61.42	2.12

TABLE VIII (continued)

Component	Retention Time (min)	Area Percent
$nC^{=}_{18}$	64.84	0.26
nC_{18}	65.22	1.33
$nC^{=}_{19}$	68.49	0.14
nC_{19}	68.83	0.90
$nC^{=}_{20}$	71.76	0.07
nC_{20}	72.27	0.49
$nC^{=}_{21}$	75.28	0.04
nC_{21}	75.57	0.31

TABLE IX

MAJOR COMPONENTS FOR 105°F
POUR CRUDE - UNTREATED

Component	Retention Time (min)	Area Percent
nC_6	1.83	20.69
nC_7	7.93	0.34
nC_8	12.78	1.04
nC_9	14.46	1.93
nC_{10}	24.30	2.59
nC_{11}	29.95	2.95
nC_{12}	35.30	2.97
nC_{13}	40.34	2.99
nC_{14}	45.09	2.94
nC_{15}	49.57	2.96
nC_{15}	53.79	2.71
nC_{17}	57.80	2.64
nC_{18}	61.61	2.38
nC_{19}	65.23	2.48
nC_{20}	68.68	2.32
nC_{21}	71.98	2.19
nC_{22}	75.14	2.13
nC_{23}	78.16	2.18
nC_{24}	81.06	2.09
nC_{25}	83.85	2.12
nC_{26}	86.54	2.13
nC_{27}	89.13	1.97
nC_{28}	91.78	1.48
nC_{29}	94.81	1.18
nC_{30}	98.31	0.80
nC_{31}	102.43	0.59
nC_{32}	107.33	0.35
nC_{33}	113.16	0.32

TABLE X

MAJOR COMPONENTS FOR 105°F
VISBROKEN LIQUID

Component	Retention Time (min)	Area Percent
$nC_6^=$	1.68	0.03
nC_6	1.83	1.51
$nC_7^=$	7.49	0.56
nC_7	7.95	0.24
$nC_8^=$	12.17	0.64
nC_8	12.79	0.72
$nC_9^=$	17.78	0.75
nC_9	18.47	1.63
$nC_{10}^=$	23.61	0.88
nC_{10}	24.31	2.62
$nC_{11}^=$	29.29	0.83
nC_{11}	29.97	3.32
$nC_{12}^=$	34.68	0.79
nC_{12}	35.33	3.56
$nC_{13}^=$	39.77	0.64
nC_{13}	40.37	3.65
$nC_{14}^=$	44.56	0.69
nC_{14}	45.12	3.60
$nC_{15}^=$	49.07	0.52
nC_{15}	49.60	3.56
$nC_{16}^=$	53.34	0.46
nC_{16}	53.83	3.27
$nC_{17}^=$	57.37	0.56
nC_{17}	57.84	3.12
$nC_{18}^=$	61.21	0.37
nC_{18}	61.64	2.81
$nC_{19}^=$	64.86	0.35
nC_{19}	65.26	2.87
$nC_{20}^=$	68.33	0.34

TABLE X (Continued)

Component	Retention Time (min)	Area Percent
nC_{20}	68.71	2.62
$nC^{=}_{21}$	71.65	0.24
nC_{21}	72.01	2.42
$nC^{=}_{22}$	74.82	0.22
nC_{22}	75.16	2.33
$nC^{=}_{23}$	77.87	0.18
nC_{23}	78.19	2.31
$nC^{=}_{24}$	80.78	0.16
nC_{24}	81.09	2.23
$nC^{=}_{25}$	83.59	0.18
nC_{25}	83.89	2.25
$nC^{=}_{26}$	86.29	0.09
nC_{26}	86.57	2.14
$nC^{=}_{27}$	88.89	0.08
nC_{27}	89.16	2.10
$nC^{=}_{28}$	91.51	0.10
nC_{28}	91.82	1.58
$nC^{=}_{29}$	94.54	0.07
nC_{29}	94.85	1.27
$nC^{=}_{30}$	98.00	0.02
nC_{30}	98.36	0.83

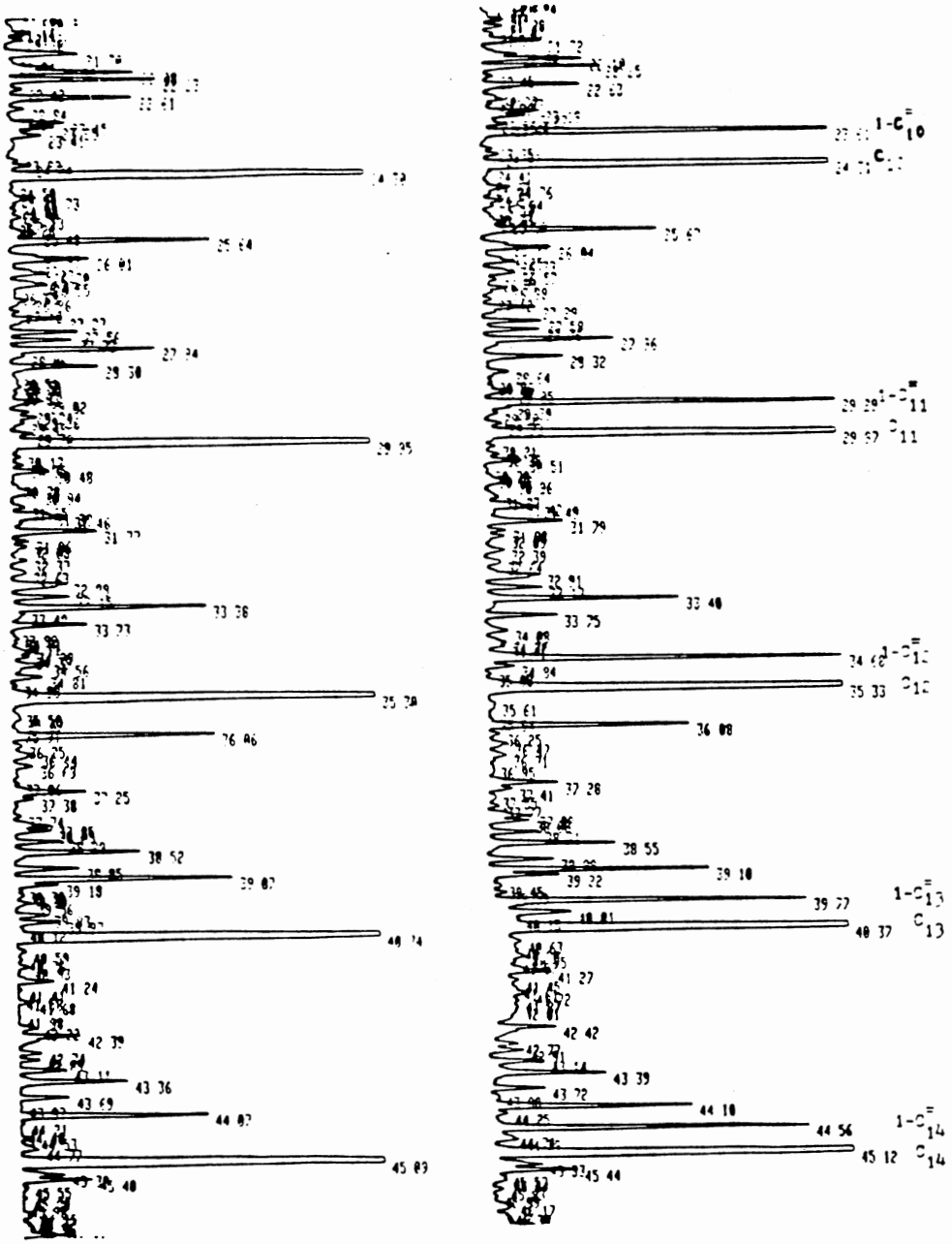

A (Untreated Crude)

B (Treated Crude A
T = 600°C, τ = 0.8 sec)

Figure 11. Chromatogram of Feedstock and Visbroken Liquid

Elemental Analyzer for the crudes and all liquid products. They are listed in Tables IV and V for whole crudes A and B and their thermally treated liquid products, respectively. A carbon/hydrogen weight ratio of 6.08 was noted for crude A with the thermally treated products exhibiting a carbon/hydrogen weight ratio range of 5.82 to 6.27. Whole crude B had a ratio of 5.95 with its treated products having a range of 5.87 to 6.49. No significant pattern between treated and untreated crudes was established.

On a total of twenty-five experiments, seven replicate runs were made. For the variables studied, it was found for duplicate or triplicate analyses, the gas composition at equilibrium varied only ±2.6% as shown in Figures 3 and 4. The total gas formed varied a maximum of ±7%. This maximum was calculated from a triplicate analysis shown in Figure 5. Duplicate runs at lower temperatures in Figures 5 and 6 show a much smaller variation. Coke formation, in Figure 7, shows a maximum variation of ±9%, with all other duplications (Figures 7 and 8) being less than this. The pour points usually had no variation and were repeated twice for each sample. On replicate runs, the pour point usually was the same, but on one replicate it was +5°F. However, the ASTM D-97 method has an inherent bias in the way the pour point is recorded, which can be at most 5°F too high.

On all experimental runs, a material balance was made. The balance closed to within ±1.6% which is a good indication of the method of operation.

CHAPTER V

DISCUSSION, CONCLUSIONS AND RECOMMENDATIONS

Discussion

While the thermal cracking of hydrocarbons has been studied for many years, the emphasis has been placed on understanding the decomposition of low molecular weight substrates (27, 28, 29). Only a few samples of thermal cracking of heavy hydrocarbons are documented in the literature (30, 31, 32, 33). The experiments described in this work are an attempt to extend that understanding to more practical applications; the pour point reduction of heavy crudes by thermal cracking. By correlating the properties and by-products of the thermally cracked heavy crudes with the severity of the heat treatment, one should be able to relate this work with that which has preceeded it and check for similarities.

Attempts to correlate the products from thermal treatment of hydrocarbon feedstocks with some combination (usually empirical) of the reaction conditions have resulted in what are called severity factors. Severity factors combine the reaction temperatures and space times in a mathematical way which can then be used to compare product data from various combinations of reaction conditions. For a given cracking severity, the yield of a final product is a function of the time-temperature-pressure response of the reactor (34). One of the first useful empirical value of a severity factor, SF, for the time-

temperature relation was given by Linden and Reid (35). They found experimentally that for the same feedstock and outlet pressure, pairs of reactor outlet temperatures and residence times lead to the same cracking severity. Their severity factor was directly proportional to the temperature and a fractional power of the space time;

$$SF = T\ \tau^{0.06}$$

where T is the temperature and τ is the space time. Many other efforts at defining a severity factor have been published. They have come in the form of equations (36,37) as above or as yields of key products or ratios of products (such as methane to ethane ratio) (11,38).

For this study, a more unique model for the severity factor was sought. The severity factor mentioned above (Linden and Reid's model) was not used because it seemed arbitrary. No derivation of it or limitations of use could be found in the literature. Other severity factors given in the literature were much more complicated. We attempted to derive a simple model which would correlate well with data already in the literature. However, graphs of severity factor (using Linden and Reid's model) versus weight percent gas and coke and pour point were made and are given in Appendix D.

Any severity factor model that one calculates must intuitively take into account that as temperature and residence time increase, so does severity. Much literature describes most hydrocarbon cracking as a global or overall first order decomposition (16,17,33,40). Of course the actual thermal decomposition is a complex collection of mostly free

radical and some molecular elementary reactions. The first order expression, integrated, is

$$- \ln \frac{C_A}{C_{Ao}} = k\tau$$

where C_A is the concentration of reactant A, C_{Ao} is the initial concentration of reactant A, k is the rate constant, τ is the time of reaction. The rate constant k, can be related to the temperature by the Arrhenius equation,

$$k = k_o e^{-E/RT}$$

where k_o is the frequency factor, E is the activation energy, T is the temperature and k is the rate constant. Substituting and defining a new severity factor, the following is obtained:

$$FC = \tau \cdot e^{-E/RT}$$

where FC is defined as

$$SF = FC = - \frac{1}{k_o} \ln \frac{C_A}{C_{Ao}} = \tau \frac{k}{k_o}$$

This definition incorporates the time of reaction as a linear effect plus temperature as an exponential effect, both relationships suggested by the generally observed first order kinetics. This model also predicts that at zero severity factor no products are created. To use our SF, an activation energy is required, and for this work, the

activation energy was assumed to be 30 kcal/mole. This value is based on previous experimental and kinetic data which have been taken in the laboratory on the pyrolysis of whole crudes and also from a comparison of pure compounds of known activation energies (39).

In the calculation of the severity factor one must use the space time, which at first appears to be easily calculated. However, for complex, poorly defined feeds (such as crudes), this is not so. Usual reaction engineering practice defines one form of space time as:

$$\tau = \frac{V_R}{v}$$

where V_R is the reactor volume and v is the volumetric flow rate of the feed defined at any arbitrary conditions. Care must be taken in defining both of these quantities for the reactor system used.

Since the laboratory reactor is not ideally isothermal, one must define an equivalent reactor volume. In experimental operations, a constant temperature throughout the length of a flow reactor is difficult to maintain. Because of this, isothermal conditions must be approximated as closely as possible. Where relatively small temperature differences exist, satisfactory results can be obtained by calculation of an equivalent reactor volume of the reactor. An equivalent reactor volume, V_R, is defined as the volume which gives, at a constant reference temperature T_R, the same conversion as the actual reactor volume with its varying temperature profile (40):

$$-r_R \, dV_R = -r dV$$

$$V_R = \frac{1}{\exp\left(\frac{-E}{RT_R}\right)} \int_0^V \exp\left(\frac{-E}{RT}\right) dV$$

where E is the activation energy defined previously. The individual experimental temperature data were measured stepwise ($\Delta\ell$ = 2.54 cm) through the length of the reactor. A typical temperature profile is given in Figure 12. The reference temperature was chosen as the equilibration temperature. Detailed calculations of the equivalent reactor volume are given in Appendix E. The actual calculated volume of the reactor was 4.98 cm^3 (0.304 in^3) based on the heated zone. At 400°C, the equivalent reactor volume had decreased to 4.20 cm^3 (0.256 in^3), at 500°C to 3.54 cm^3 (0.216 in^3), and at 600°C to 3.29 cm^3 (0.201 in^3).

According to Levenspiel (41), one usually measures the volumetric flow rate at some standard state, especially when the reactor is to operate at a number of temperatures. If the material is a gas when fed to the reactor but is liquid at the standard state, one must specify precisely what standard state has been chosen. Because of this, the volumetric flow rate was adjusted to account for the mixed vapor-liquid nature of the feed at the reactor temperatures. This was done using the ASTM D-1160 distillation curve. For Crude A at 400°C approximately 20% is vaporized; at 500°C, 38% and at 600°C, 55%. For crude B at 400°C, 5% is vaporized; at 500°C, 15%, and at 600°C, 25% is vaporized.

Having defined all critical variables, the severity factors were calculated. Tables XI and XII lists the severity factors and conditions for crude A and crude B respectively. Figure 13 shows the effect of the severity on the amount of gas produced for both crudes. Figure 14 shows the same for crude A but expanded to show lower SF value details.

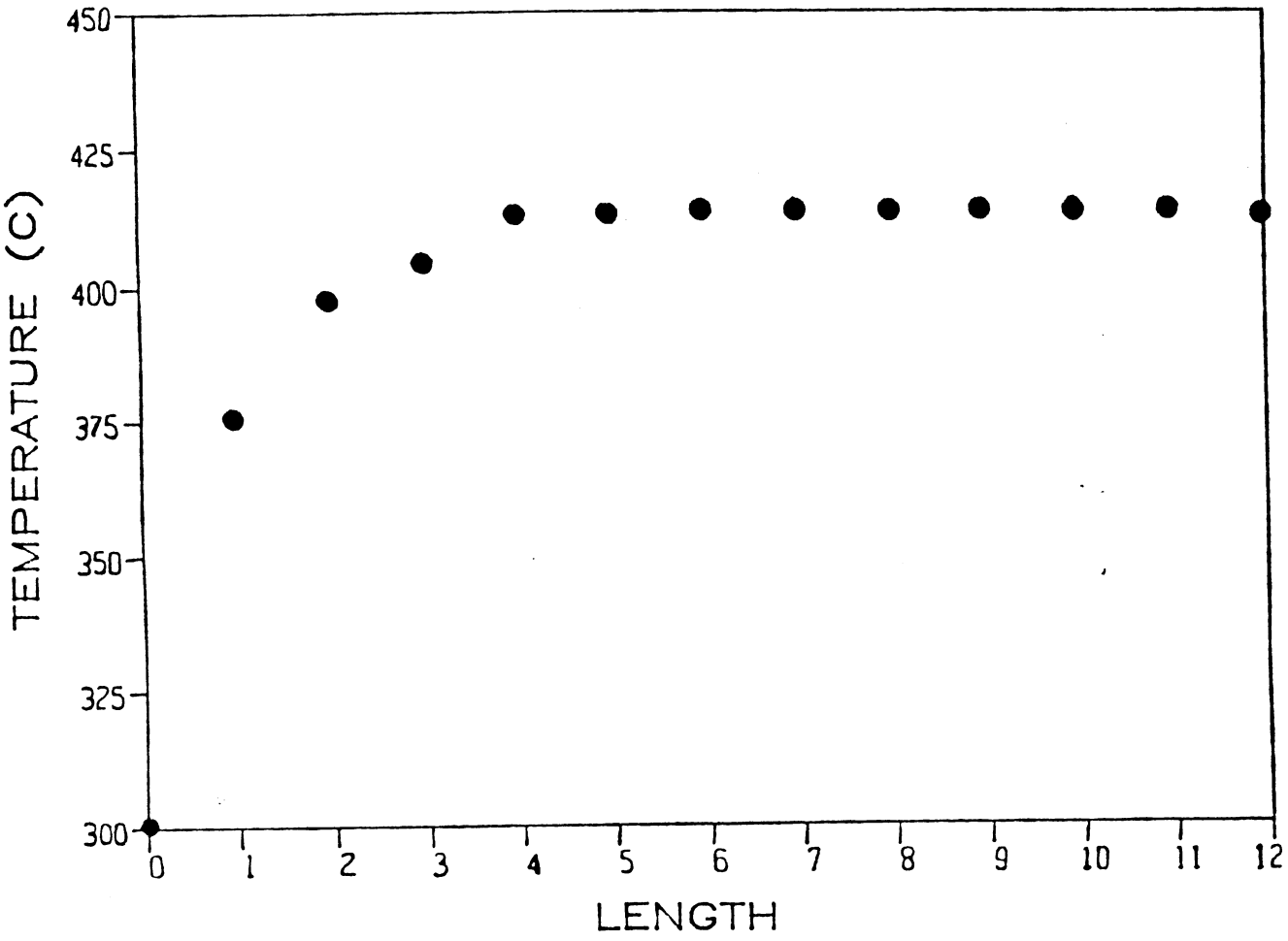

Figure 12. Temperature Profile of Reactor at 400°C

TABLE XI

SEVERITY FACTOR SF* - CRUDE A

Temp. (°C)	Flow (ml/min)	Space Time (s)	Severity Factor x 10^{-10} (s)
400	3.9	0.8	1.94
400	1.6	2.14	8.64
400	0.8	3.56	12.3
500	3.9	0.27	13.2
500	1.6	0.67	41.6
500	0.8	1.57	93.8
600	3.9	0.15	44.5
600	1.6	0.44	165
600	0.8	0.79	267

*$SF = \tau e^{-E/RT}$

TABLE XII

SEVERITY FACTOR SF* - CRUDE B

Temp. (°C)	Flow (ml/min)	Space Time (s)	Severity Factor x 10^{-10} (s)
400	3.9	3.13	5.66
400	1.6	7.3	19.5
400	0.8	14.3	43.4
500	3.9	0.8	36.8
500	1.6	1.5	57.4
500	0.8	5.5	82.8
600	3.9	0.5	198
600	1.6	1.1	397
600	0.8	2.6	1030

*$SF = \tau e^{-E/RT}$

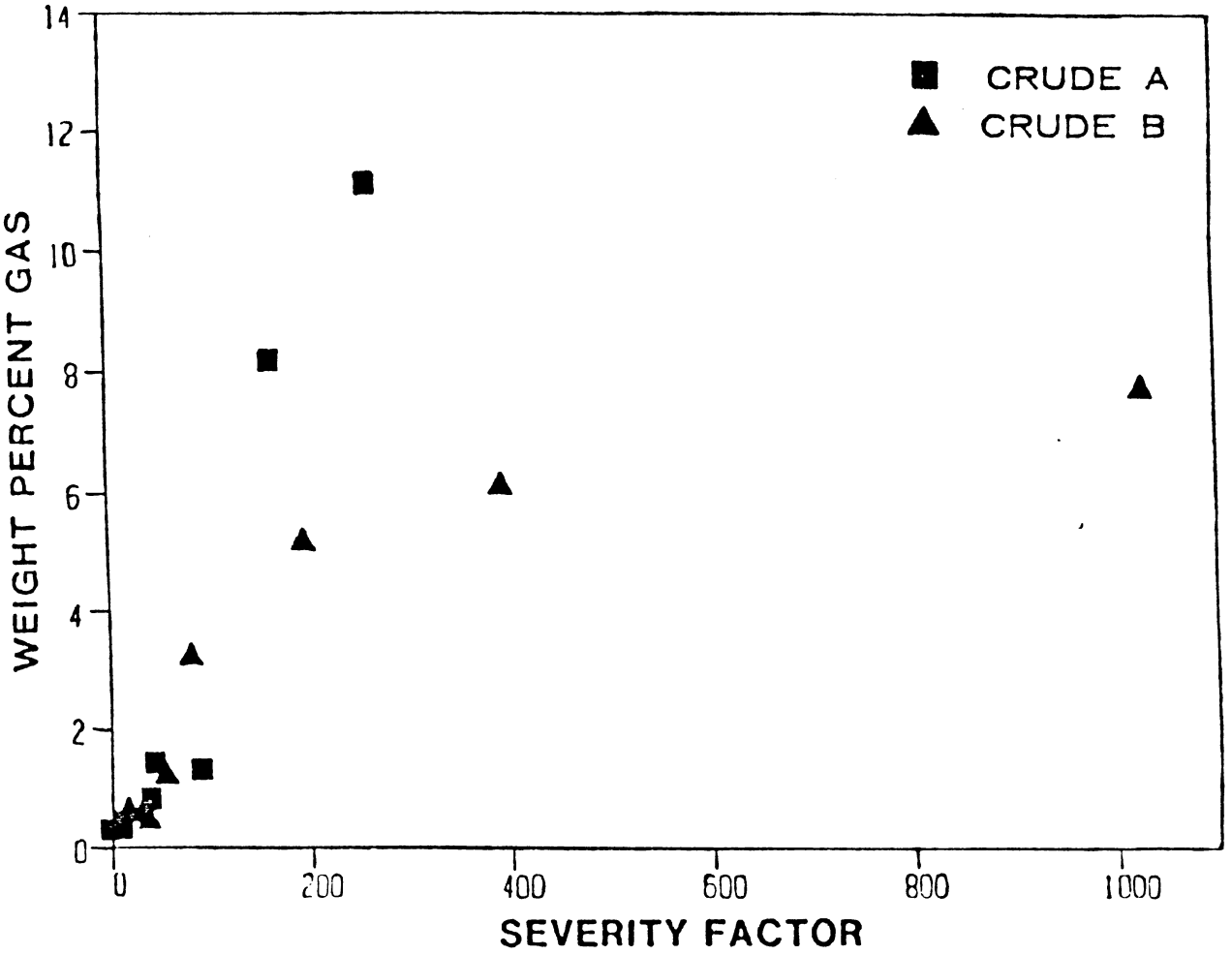

Figure 13. Weight Percent Gas Formed as a Function of Severity Factor - Crudes A and B

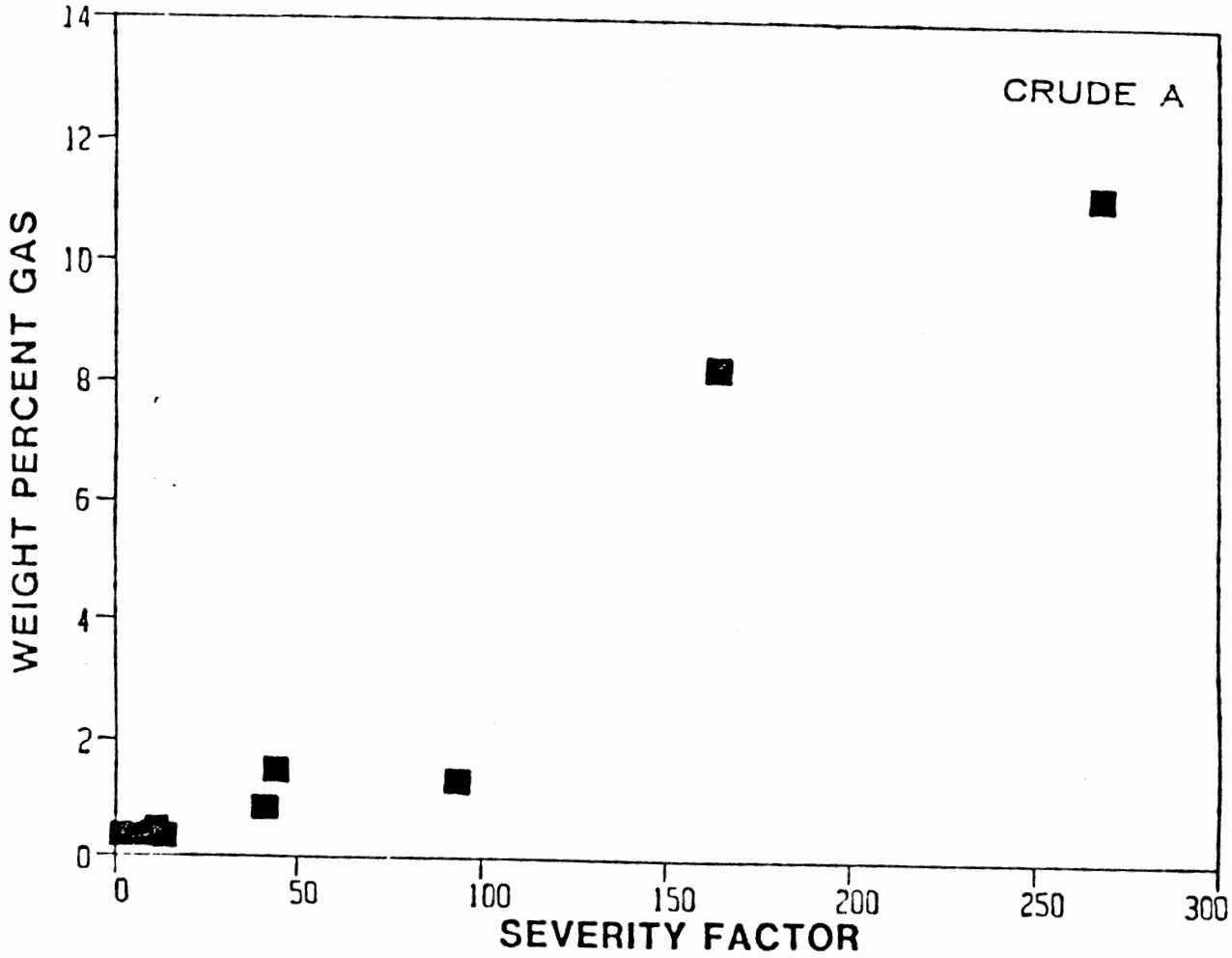

Figure 14. Weight Percent Gas Formed as a Function of Severity Factor - Crude A

Figure 15 shows the effect of severity factor on the amount of coke formed for both crudes. Figure 16 shows the effect of severity factor on pour point reduction for crude A, again to show lower value details; and Figure 17 shows the same for both crude A and crude B.

Inspection of these figures shows the amount of either gas or coke formed increases rapidly as severity factor increases. However, the amount of gas formed begins to level off at severity factors greater than 400 s for crude B. Crude A produces much more gas but severity factors greater than 300 were not obtained. This is due to the relationship between the nature of the crude and the calculation of space time (which in turn affects the severity factor). The crudes were compared at the same set of conditions and differences between the crudes caused different space times and, hence, severity factors. Zdonik et. al. (33), showed similar behavior in gas yield versus cracking feedstock severity. Even though their cracking severity was calculated differently, the curve took on a similar shape.

Coke formation shows similar behavior. For both crudes, the coke formed increases rapidly as severity factor increases and then begins to level off. Crude B forms significantly more coke. This could have been predicted from its ASTM distillation curve and conradson carbon content. By a comparison of distillation curves, crude B formed much less vapor than crude A which may tell of its coking capability. Also, crude B has a significantly higher conradson carbon content. The value of the conradson carbon content can be used as a measure of how the crude will coke. The higher the conradson carbon content means higher coke formation.

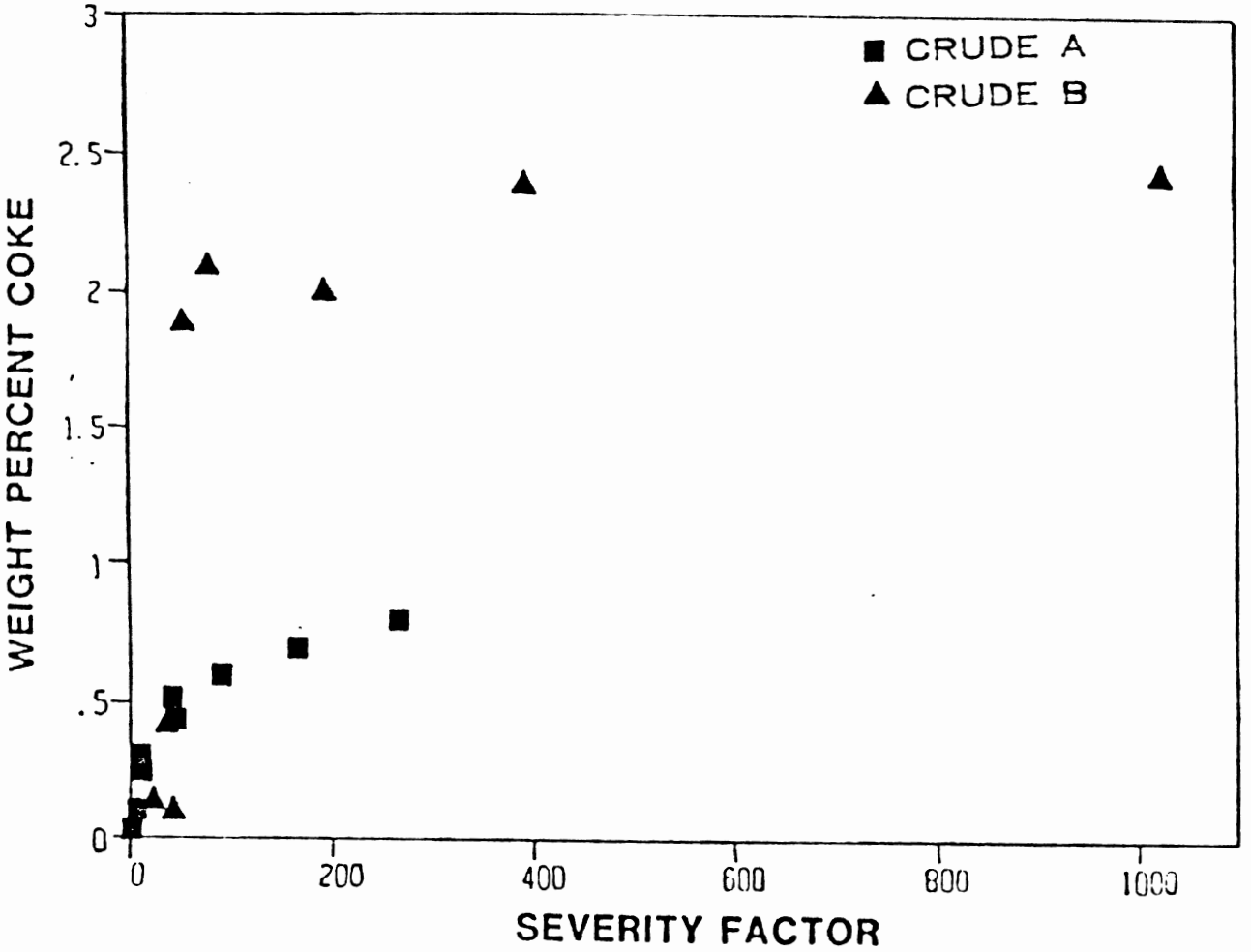

Figure 15. Weight Percent Coke Formed as a Function of Severity Factor - Crudes A and B

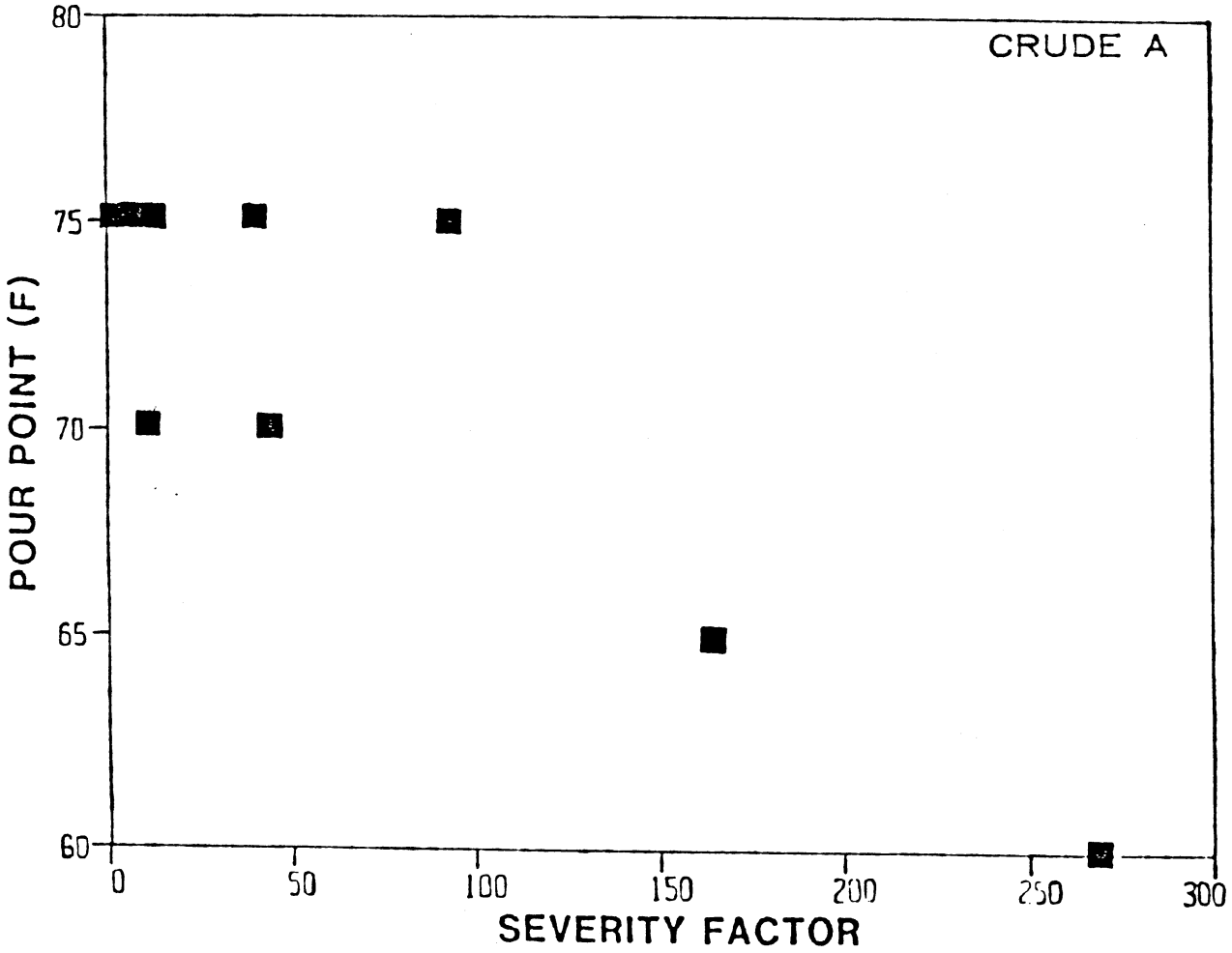

Figure 16. Pour Point as a Function of Severity Factor - Crude A

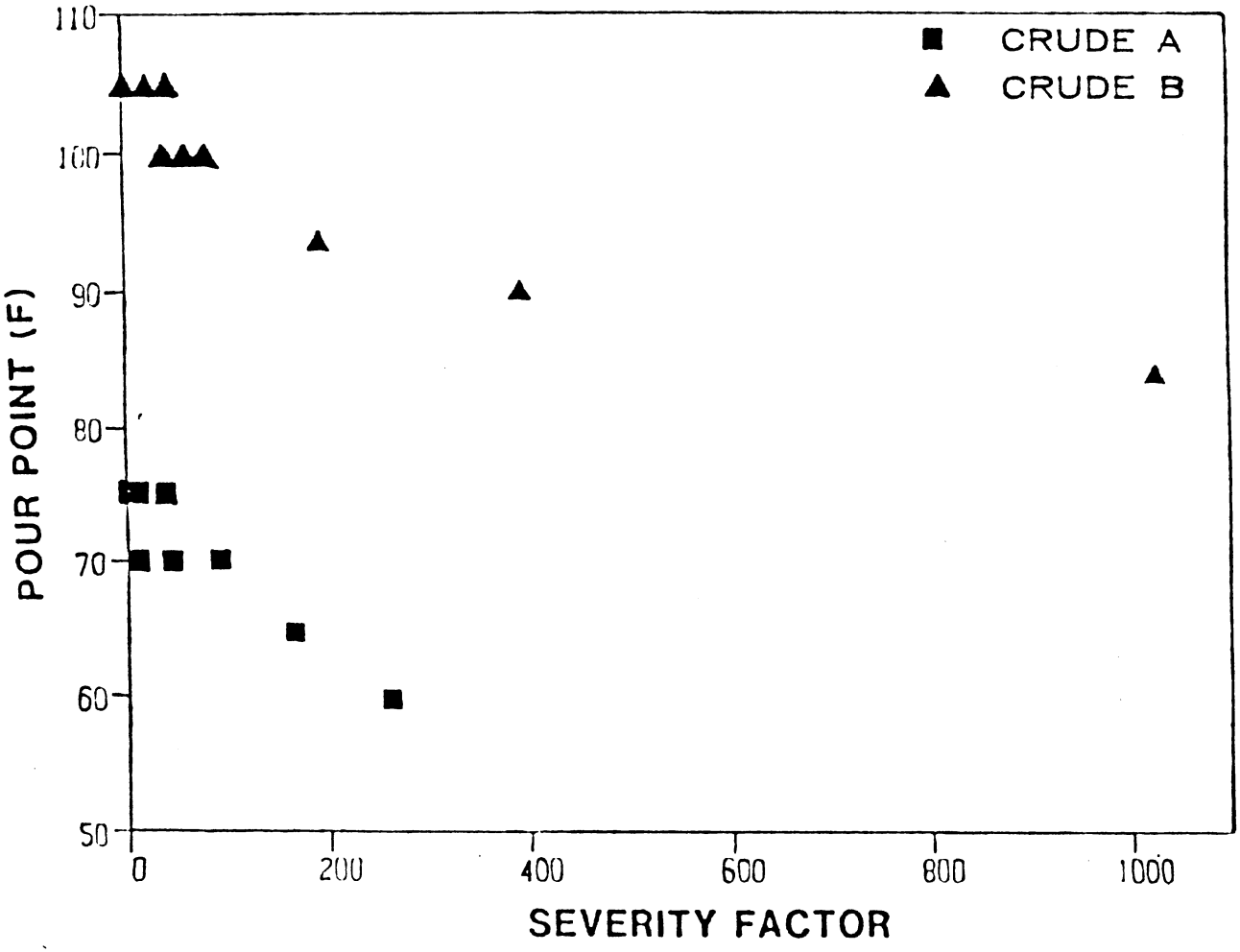

Figure 17. Pour Point as a Function of Severity Factor - Crudes A and B

The effect of severity factor on pour point shows that as the severity factor increases, the pour point decreases. For crude A, an almost instantaneous 5°F decrease in pour point occurs as soon as the severity factor increases. Crude B is not quite as sensitive but also quickly decreases as severity factor increases. Since crude B's properties allowed for testing over a wider range of severity factors, one can see that the decrease in pour point eventually levels off. Beyond SF of 1000 little reductions in pour point can be achieved. Crude A, which did not allow a wide range of severity factors shows only decreasing pour points. Since experiments were conducted at identical conditions for both crudes, it is interesting to note that a 20°F reduction in pour point is observed for both crudes.

The general responses of the gas yield, coke and pour point versus severity factor curves show that our new SF (FC) is a reasonable relationship for predicting responses by combining reaction temperature and time. The SF (FC) is based upon first order, global reactions and remains relatively simple to use.

During the latter course of this study, a fused silica capillary column GC analysis was performed on each of the whole crudes and one of their visbroken products. The objective was to obtain preliminary data on how reduction in pour point is achieved. A more indepth study was done by Zhou and Crynes (42). The products chosen for capillary analysis were those treated at the most severe conditions, 600°C and 0.79 mℓ/min. For crude A, this translates to a severity factor of 267 s, and for crude B, a severity factor of 1030 s.

For both crudes, a similar phenomenon occured. No way was available to determine how much of the total crude was vaporized to the

chromatograph column from the injection zone. The chromatograph area percent ratio of alkenes to alkanes (for each carbon number) steadily decreased as carbon number increased for the visbroken liquid. Tables XIII and XIV give the alkene/alkane area percent ratios for crude A and B, respectively. On the whole crude chromatograms, the only major peaks were those of the respective normal paraffins. However, on the chromatograms of the visbroken liquids, there was a matched peak pair: the peaks for the C_n alkenes plus that for the C_n alkanes. These alkenes were always the alpha-olefin peak followed by the normal paraffin peak. This phenomenon occured identically for both crudes. This occurence has been seen in other research work conducted in our laboratories. Zhou and Crynes in their article (43), noted this same response, i.e. $C_7 + C_7^{=} > C_8 + C_8^{=} > C_9 + C_9^{=} >$, etc. for n-dodecane thermolysis. According to Rebick (33), straight-chain paraffins produce only straight-chain products, and all olefins produced are alpha olefins. Additionally, olefins are the main products of paraffin pyrolysis. This results from the complex free radical mechanism of the decomposition of crude oils.

Measurement of the carbon/hydrogen weight ratio of both the whole and visbroken crudes should have confirmed this loss in hydrogen; from normal alkane to 1-alkene. Attempts to show this, however, were unsuccessful as listed in Tables IV and V for crudes A and B. In fact, no noticeable change occurred. Interestingly, Krishnamurthy, Shah, and Stiegel monitored an H/C atomic ratio for a crude treated at 600°C for various residence times and showed that no appreciable change in the ratio occured. Only at higher temperatures were significant changes observed (44). In retrospect, this may have actually been predicted

TABLE XIII

ALKENE/ALKANE RATIO FOR CRUDE A - VISBROKEN LIQUID

Carbon Number	Area Percent Ratio
6	20.3
7	5.0
8	2.33
9	1.58
10	1.16
11	0.74
12	0.49
13	0.33
14	0.33
15	0.24
16	0.22
17	0.20
18	0.19
19	0.16

TABLE XIV

ALKENE/ALKANE RATIO FOR CRUDE B - VISBROKEN LIQUID

Carbon Number	Area Percent Ratio
6	2.35
7	0.89
8	0.46
9	0.34
10	0.25
11	0.22
12	0.17
13	0.19
14	0.15
15	0.14
16	0.18
17	0.13
18	0.12
19	0.13
20	0.10
21	0.09
22	0.08
23	0.07
24	0.08
25	0.04
26	0.04
27	0.06
28	0.06
29	0.04

because of the heavy nature of the crude. Since the whole crudes contain such a large percentage of high carbon number alkanes, measuring any significant loss in hydrogen stretches the limits of accuracy of the elemental analyzer. For example, a high carbon number alkane, losing only two hydrogen atoms to form a 1-alkene forces the analysis to be accurate to many significant digits. For instance, conversion of n-C_{30} paraffin to n-C_{30} olefin involves a change in carbon/hydrogen ratio of from 30/62 (0.484) to 30/60 (0.5); a very small change (3%).

From the general stoichiometry a few observations can be made. For a crude which makes much gas (rich in hydrogen) and little coke one would expect the C/H weight ratio to increase. Alternatively, for a crude which makes much coke (carbon rich) and not much gas, one would expect the ratio to decrease.

By considering the melting points of alkanes and alkenes, one can rationalize the reduction in pour point of the crudes. A comparison of the melting points of paraffins and the corresponding alpha olefins is given in Table XV. This shows that the alkenes (up to C_{30}) have lower melting points than their alkane counterparts. The whole crudes have high pour points because they contain significant amounts of n-paraffins. The pour point decreases after thermal treatment because of the production of alpha-olefins which have lower melting points than the n-paraffins. The alpha-olefins have lower melting points, especially so for those with lower carbon numbers, i.e. the difference between the melting points is greater, the lower the carbon number. These olefins could tend to act as solvents for the higher alkenes and alkanes, therefore also reducing the pour points. Also, in the global cracking process the quantity of the total alkanes and alkenes are shifted down

TABLE XV

MELTING POINTS OF n-PARAFFINS AND THEIR CORRESPONDING 1-OLEFINS

Compound	Melting Point (°C)[1]
C_7	-90.6
$C_7^=$	-119.2
C_8	-59.8
$C_8^=$	-102.4
C_{10}	-29.7
$C_{10}^=$	-66.3
C_{11}	-25.59
$C_{11}^=$	-49.19
C_{12}	-9.6
$C_{12}^=$	-35.23
C_{13}	-5.5
$C_{13}^=$	-13.0
C_{14}	5.86
$C_{14}^=$	-12.0
C_{15}	10.0
$C_{15}^=$	2-8
C_{16}	18.7
$C_{16}^=$	4.1
C_{20}	36.8
$C_{20}^=$	28.5
C_{30}	65.8
$C_{30}^=$	62-63

[1]From Handbook of Chemistry and Physics, 54th Edition, 1973-1974, Robert Weast Editor in Chief

to lower carbon numbers. Hence, a double effect occurs; more alkenes relative to alkanes and generally lower carbon numbers.

Conclusions and Recommendations

The results presented here illustrate the feasibility of reducing the pour point of high pour point whole crudes by simple thermal treatment. The reaction products from this treatment (coke and gas) have been shown to relate directly with a new severity factor which can be developed from a first order global decomposition model.

The reduction in pour point has been shown to correlate with a definite chemical change in the composition of the crude. Capillary gas chromatography has shown that the thermal treatment converts the normal paraffins of the whole crude to normal alpha alkenes in the visbroken crude. Practical application of this process in a refinery would result in much less gas formation and comparable coke formation.

Below are the conclusions which can be drawn from this study:

1. Concentration of hydrocarbon gases reached an equilibrium value after 30 minutes of thermal treatment.
2. Both crudes show the same characteristic curves of total gas formation. As temperature increases, so does gas production. At low temperatures, gas production does not increase significantly when space time increases. However, at high temperatures, the gas production increases rapidly as space time increases.
3. Both crudes show the same characteristic curves of total coke formation. As temperature increases, so does coke formation. At low temperatures, coke formation is not significant as space

time increases. However, at high temperatures, coke formation increases as space time increases.

4. A maximum 20°F decreases in pour point could be attained at the conditions studied. The reduction in pour point for both crudes depends most strongly on space time at the highest temperature studied.

While our work shows the feasibility of treating whole crudes in the manner described, additional experiments to further define the application of this process are warranted.

Listed below are recommendations for potential further work on this project:

1. Research a wider range of pour point crudes and study the pour point reduction effect. The crudes here had a fairly wide range of pour point but were similar in nature, as shown by the carbon/hydrogen ratio. It may be interesting to start with a crude of a high carbon/hydrogen ratio (9 or 10) and observe the effects of visbreaking.
2. Further studies on the GC need to be done in order to better understand what is happening during the visbreaking process. These studies have been started in our laboratory with various types of feedstocks. They include pure compounds, a mixture of two compounds, and a synthetic mixture of six compounds. All visbroken products are being analyzed by the GC to better understand the selective process towards alpha-olefins.
3. The most interesting recommendation is to do an analysis of pour point reduction as a function of reactor time on stream. That is, to see how the pour point of the first drop of crude out of

the reactor compares with that of the last drop out of the reactor; and drops at preselected times in between. Because of the small volume of material to be measured, a technique such as differential scanning calorimetry (DSC) would probably have to be used. It has been noted in the literature that DSC can be used to determine a rough estimate of the pour point with good accuracy. This recommendation was made because a significant difference in the color of the drops was observed during the course of the thermal treatment. The drops, especially for crude B, changed drastically in color, from black to gold, during the duration of the experiment.

4. Remove the light ends of a whole crude (by distillation) and treat the remainder of the crude by the method described here. This would represent a realistic situation in a refinery equipped with a visbreaker unit where the feed for the visbreaker unit is the residual crude which has gone through a demethanizer, deethanizer, depropanizer, and so forth.

REFERENCES

1. Schuetze, B., Hofmann, H., Hydrocarbon Processing, 63, (2), 75 (1984).

2. Allen, J. G., Little, D. M., Waddill, P. M., Petroleum Refiner, 30, (7), 107 (1951).

3. Dubbs, Jesse A., U. S. Patent 1002570.

4. Stolfa, Frank, Hydrocarbon Processing, 59, (5), 101 (1980).

5. Jahnig, C. E., "Refinery Processes Survey", in Kirk - Othmer Encyclopedia Chemical Technology, Vol. 17, p. 189.

6. Jahnig, C. E., Martin, H. Z., Campbell, D. L., ChemTech, 14, (2) 106 (1984).

7. The Oil and Gas Journal, 76 (45), 56 (1978).

8. Yepsen, G. L., Jenkins, J. H., Hydrocarbon Processing, 60, (9), 117 (1981).

9. Hournac, R., Kuhn, J., Notarbartolo, M., Hydrocarbon Processing, 58, (12), 97 (1979).

10. Notarbartolo, M., Menegazzo, C., Kuhn, J., Hydrocarbon Processing, 58, (9), 114 (1979).

11. Allen, D. E., Martinez, C. H., Eng., C. C., Barton, W. J., Chemical Engineering Progress, 79, (1), 85 (1985).

12. Akbar, M., Geelen, H., Hydrocarbon Processing, 60, (5), 81 (1981).

13. Heavy Oil Processing Handbook, The Chemical Daily Company, Ltd., Tokyo, Japan, 1982.

14. The Oil and Gas Journal, 48 (46), 183 (1950).

15. Nelson, W. L., The Oil and Gas Journal, 67, (45), 229 (1969).

16. Rhoe, A., de Blignieres, C., Hydrocarbon Processing, 58, (1), 131 (1979).

17. Hus, Martin, The Oil and Gas Journal, 79, (15), 109 (1981).

18. Speight, James C., The Chemistry and Technology of Petroleum, Marcel Dekker, Inc., New York, 1980.

19. Beuther, H., Goldthwait, R. E., Offutt, W. C., The Oil and Gas Journal, 57, (9), 151 (1959).

20. Russell, R. J., Chapman, E. D., Journal of the Institute of Petroleum, 57, (554), 117 (1971).

21. Mukhopadhyay, Asim K., Pipeline Industry, 50, (6), 55 (1979).

22. Dikshit, R. D., Datta, P., Chaliha, S., Chemical Engineering World, 14, (1), 77 (1979).

23. Irani, C., Zajac, J., Journal of Petroleum Technology, 34, (2), 289 (1982).

24. Holder, G. A., Winkler, J., Journal of the Institute of Petroleum, 51, (449), 228, (1965).

25. Fujita, N., Fumagai, Y., Shoji, Y., Kubo, H., Maruyama, T., Chemical Engineering Progress, 79, (1), 76 (1983).

26. Wing, Milt, ChemTech, 10, (1), 20 (1980).

27. Back, M. H., Back, R. A., "Thermal Decomposition and Reactions of Methane", in Pyrolysis: Theory and Industrial Practice, Lyle F. Albright, Billy L. Crynes, William H. Corcoran (Eds), Academic Press, New York, 1983, pg. 1.

28. McConnell, C. F., Head, B. D., "Pyrolysis of Ethane and Propane", in Pyrolysis: Theory and Industrial Practice, Lyle Albright, Billy L. Crynes, William H. Corcoran (Eds), Academic Press, New York, 1983, pg. 47.

29. Corcoran, W. H., "Pyrolysis of Ethane and Propane", in Pyrolysis: Theory and Industrial Practice, Lyle Albright, Billy L. Crynes, William H. Corcoran (Eds), Academic Press, New York, 1983, pg. 47.

30. Voge, H. H., Good, G. M., Journal of American Chemical Society, 71, 593 (1949).

31. Fabuss, B. M., Smith J. O., Lait, R. I., Borsanyi, A. S., Satterfield, C. N., Industrial Engineering Chemical Process Design and Development, 1, 298 (1962).

32. Mushrush, G. W., Hazlett, R. N., Industrial Engineering Chemical Fundamentals, 23, 288 (1984).

33. Rebick, C., "Pyrolysis of Ethane and Propane", in Pyrolysis: Theory and Industrial Practice, Lyle Albright, Billy L. Crynes, William H. Corcoran (Eds), Academic Press, New York, 1983, pg. 69.

34. Nowak, S., Giinschel, H., "Pyrolysis of Ethane and Propane", in Pyrolysis: Theory and Industrial Practice, Lyle Albright, Billy L. Crynes, William H. Corcoran (Eds), Academic Press, New York, 1983, pg. 277.

35. Linden, H. R., Reid, J. M., Chemical Engineering Progress, 55, (3), 71 (1959).

36. Zdonik, S. B., Green, E. J., Hallee, L. P., The Oil and Gas Journal, 65, (26), 96 (1967).

37. Illes, V., Szalai, O., Csermely, A., Otto, A., Chemical Technology, 30, 122 (1978).

38. Leonard, J. J., Gwyn, J. E., McCullough, E. R., "Pyrolysis Bench Scale Unit Design and Data Correlation", in Industrial and Laboratory Pyrolysis, Lyle F. Albright, Billy L. Crynes, (Eds).

39. Crynes, B. L., Chang, C. W., Unpublished data, Oklahoma State University, 1983.

40. Hougen, O., Watson, K., Chemical Process Principles, Vol. 111, Wiley and Sons, Inc., New York, 1947, pg. 889.

41. Levenspiel, O., Chemical Reaction Engineering, (2nd Ed), Wiley and Sons, Inc., New York, 1972, pg. 101.

42 Zhou, P., Crynes, B. L., Unpublished article, Oklahoma State University, 1985.

43. Zhou, P., Crynes, B. L., "Thermolytic Reaction of Dodecane", Unpublished article, Oklahoma State University, 1985.

44. Krishamurthy, S., Shah, Y. T., Stiegel, G. J., Industrial Engineering Chemical Process Design and Development, 18, (3), 466 (1979).

APPENDIXES

APPENDIX A

EQUIPMENT AND SUPPLIES USED

The following equipment and supplies were used to carry out the experimentation described in this thesis:

Two Matheson Flowmeters Model 701-PBV

Powerstat Variable Auto Transformer 0-140 V 10 A

Omega Digital Temperature Indicator Model 400A

Four thermocouples Omega Engineering Inc. Type K Chromel-Alumel

Hewlett Packard Temperature Programmer 240

Harvard Syringe Infusion/Withdrawal Pump Series 950

Precision Scientific Company Wet Test Meter

Hewlett Packard 1-10-100 ml Soap Film Flowmeter

0.64 cm (0.25 in) copper tubing.

0.64 cm (0.25 in) brass ferruls and nuts, Parker Fluid Connectors

Hydrogen- 99.95% Purity, Air- 100%, Helium- 99.95%, Nitrogen- 99.95%, Oxygen- 99.95%

Ascarite II, 8-20 mesh, Arthur H. Thomas Company

Two ml syringe, Luer Lok Tip Becton, Dickinson and Company

Marsh Beaded Heaters 1500 W, 115 V

Thermolyne Briskheat Flexible Electric Heating Tape 120 V, 416 W 0.01 m x 2.4 m Heavy Insulated Fibrox

CALIBRATING GASES
Scotty analyzed gases (from Scott gas Products):
1. Can Mix 220
2. Can Mix 54
3. Can Mix 61
4. Can Mix 222

Scientific Gas Products:
1. 2% Methane in Air
2. 1% Ethane in Nitrogen

APPENDIX B

RELATIVE WEIGHT RESPONSE FACTORS

To determine relative weight response factors the following procedure was used.

Ten μℓ of:

1. Methane 0.1913 % by volume in air
2. Ethane 0.09855 % by volume in air
3. Propane 0.09952 % by volume in air
4. N-Butane 0.09591 % by volume in air
5. I-Butane 0.09923 % by volume in air
6. Pentane 0.1967 % by volume in air

were injected to the GC at the chosen operating conditions.

To calculate the Relative Weight Response Factor (RWRF) of the gases expected from pyrolysis:

1. Calculate volume of component in sample injected
2. Look up density of component (CRC, Chem. Eng. Handbooks)
3. Calculate weight of component (1 x 2)
4. Get area of component from GC output
5. Calculate area/weight (4/3)
6. Pick a reference component, in this case it was methane
7. Calculate RWRF as $(\text{area/weight})_i/(\text{area/weight})_r$

Since all RWRF calculated by this method of the mixture above were all very close to 1.00, the weight percent was assumed to be area percent which was a good approximation within experimental error. If the RWRF were not close to 1.00, the weight percent would have been calculated as:

$$\text{wt\% } i = \frac{A_i/RWRF_i}{\sum_{i=1}^{n} (A_i/RWRF_i)}$$

APPENDIX C

OPERATING CONDITIONS OF GAS CHROMATOGRAPHS

TABLE XVI

HP5890 GC OPERATING CONDITIONS

Type of Column	Porapalk Q
Column Length (m)	1.8
Internal Diameter (m)	2.58×10^{-3}
Column Temperature (°C)	160
Injector Temperature (°C)	160
Detector Temperature (°C)	160
Carrier Gas	He
Syringe Sample Size (μl)	50
He flow rate (ml/min)	30
H_2 flow rate (ml/min)	32
Air flow rate (ml/min)	450
Threshhold	-2
Attenuation	0-4
Peak Width	.16
Chart Speed (m/min)	0.03
Reconditioned Column	2 weeks, 200°C, 12 h

TABLE XVII

HP 5880 GC OPERATING CONDTIONS

Type of Column	Fused Silica Capillary
Column Length (m)	60
Internal Diameter (m)	0.32×10^{-3}
Column Temperature	35°C - 5 min to 270°C
Rate °C/min	5
Injector Rate Temperature (°C)	250
Detector Temperature (°C)	300
Carrier Gas	H_2
Sample Size	
H_2 flow rate (m/min)	27

APPENDIX D

SEVERITY FACTOR AS CALCULATED BY LINDEN AND REID

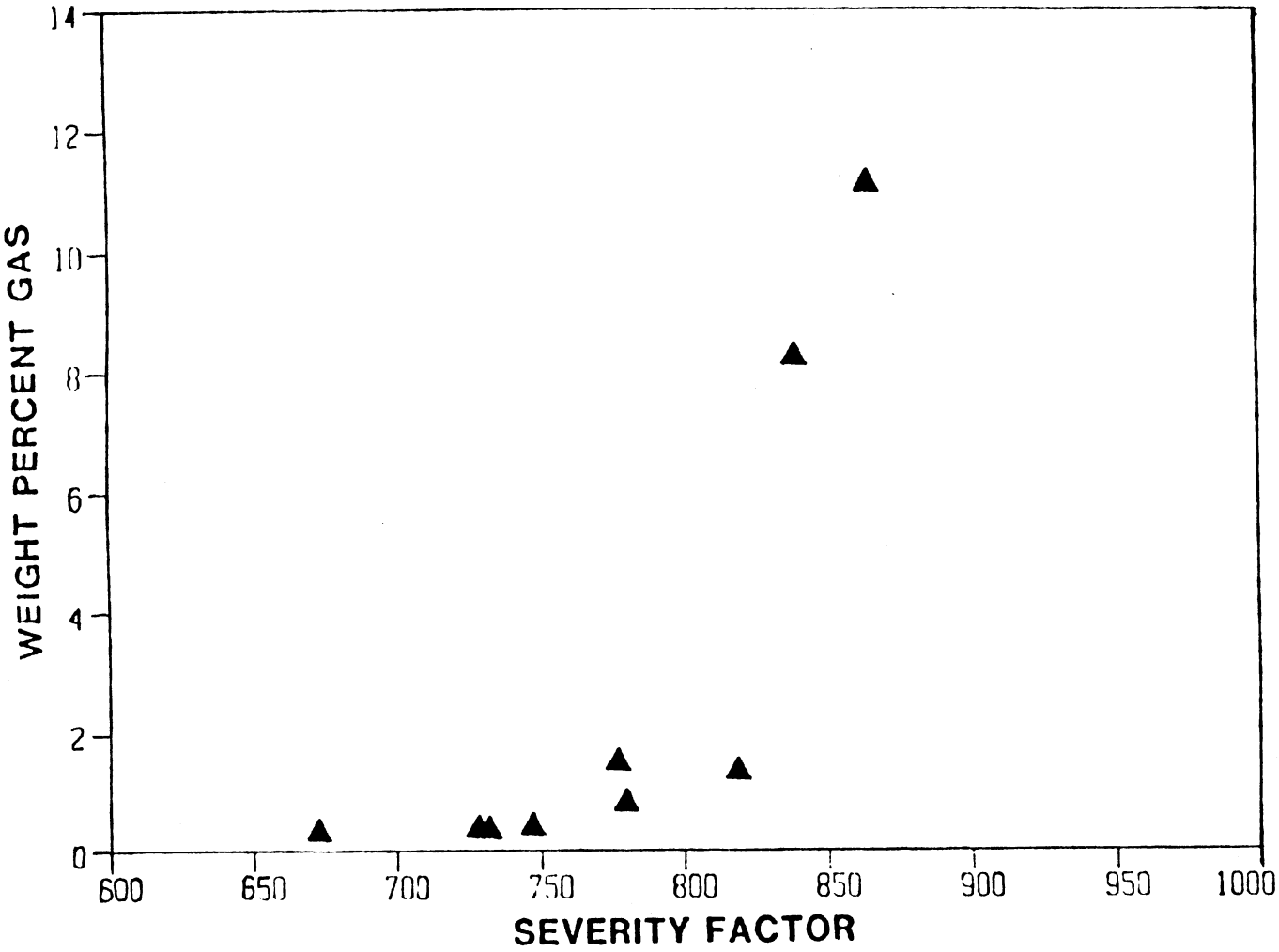

Figure 18. Weight % Gas Formed as a Function of Linden and Reid's Severity Factor - Crude A

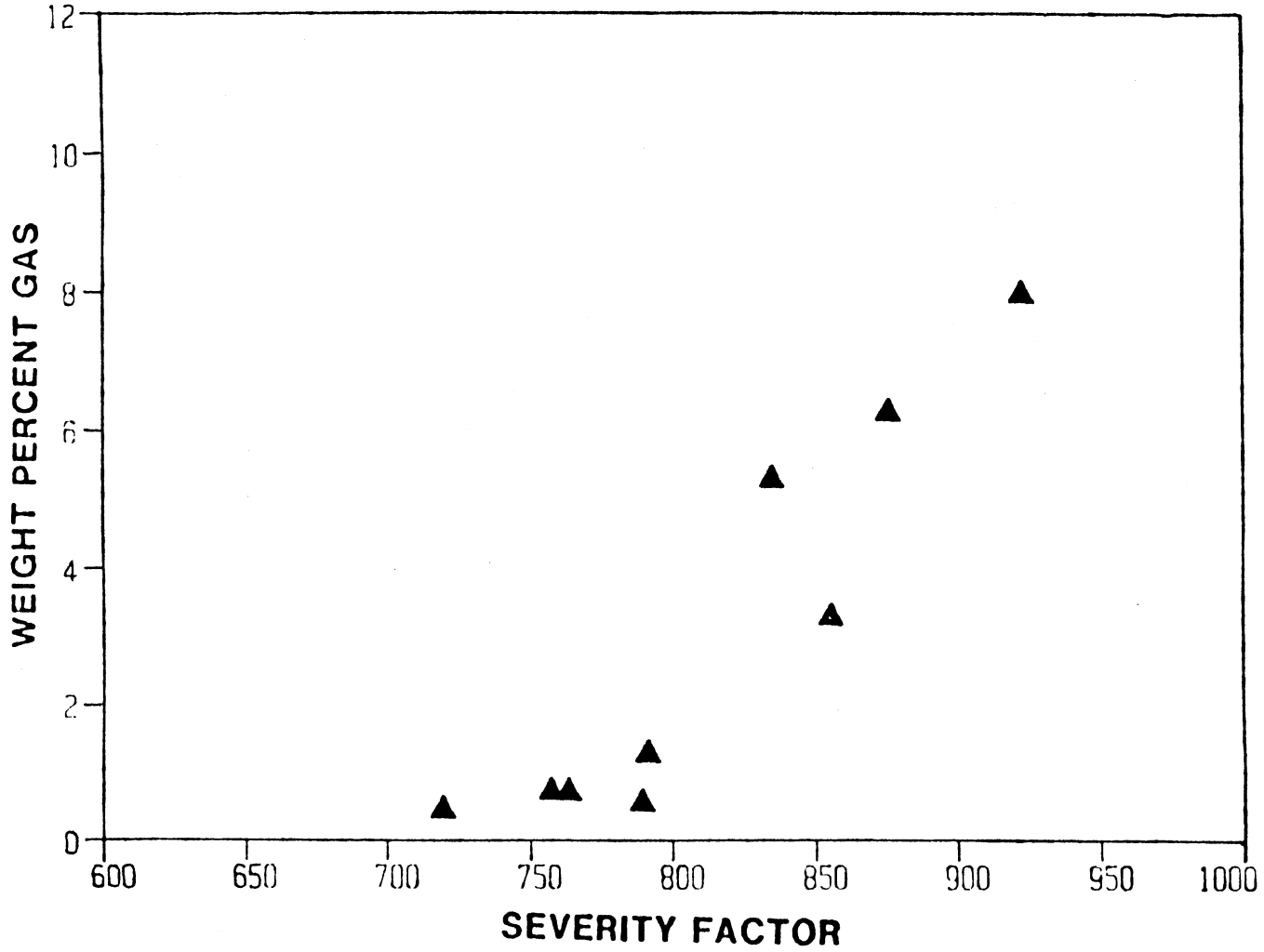

Figure 19. Weight % Gas Formed as a Function of Linden and Reid's Severity Factor - Crude B

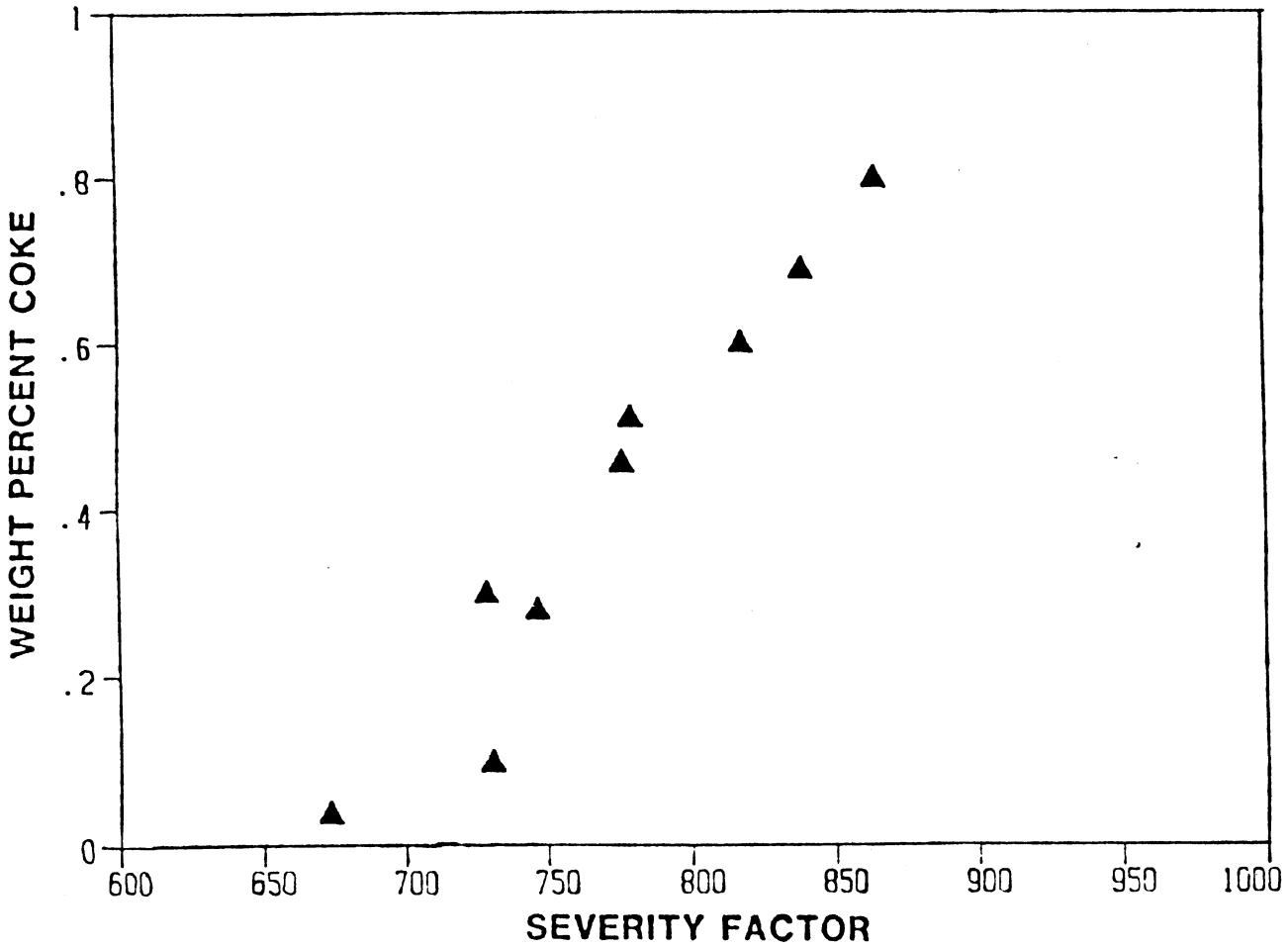

Figure 20. Weight % Coke Formed as a Function of Linden and Reid's Severity Factor - Crude A

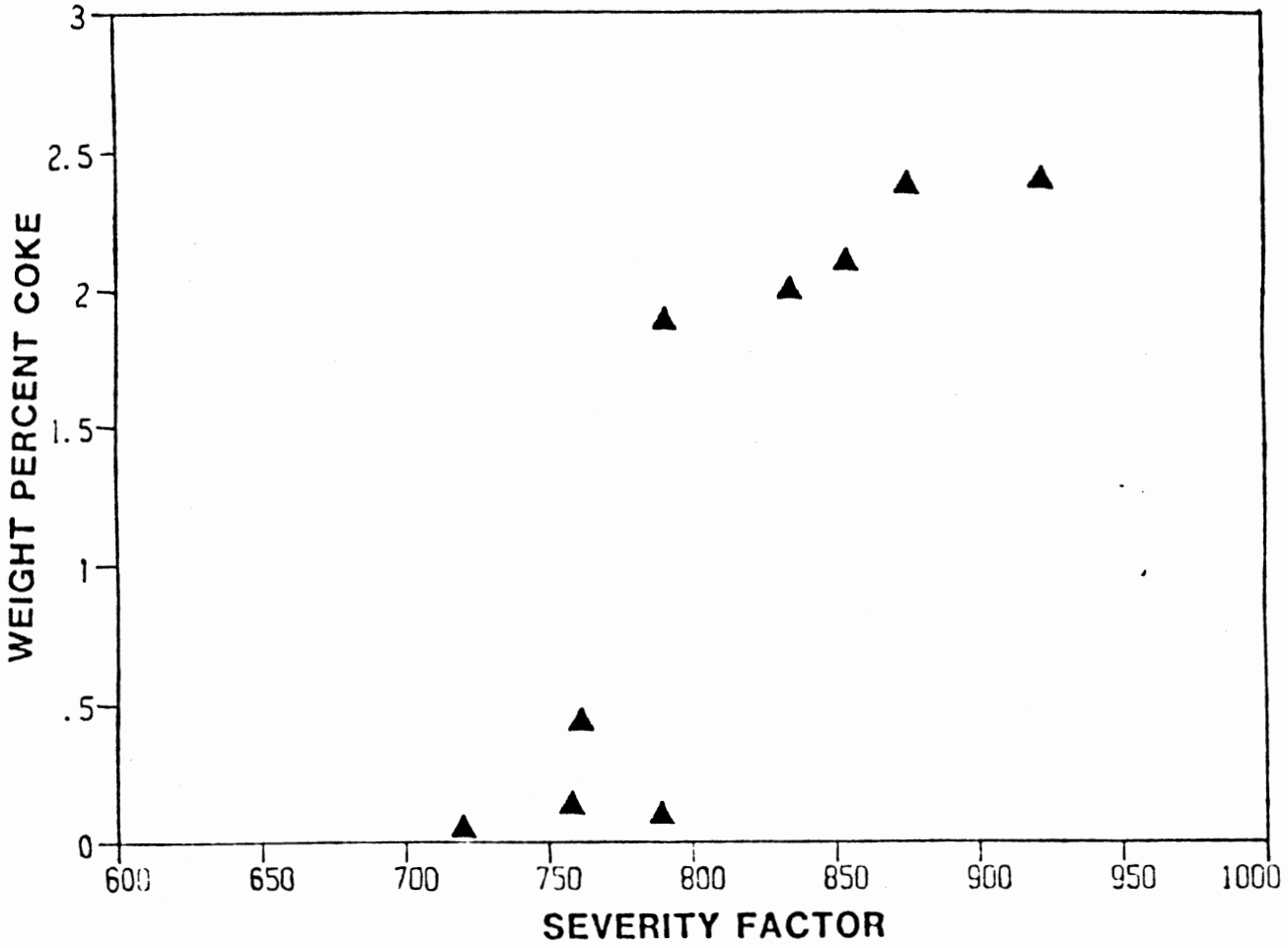

Figure 21. Weight % Coke Formed as a Function of Linden and Reid's Severity Factor - Crude B

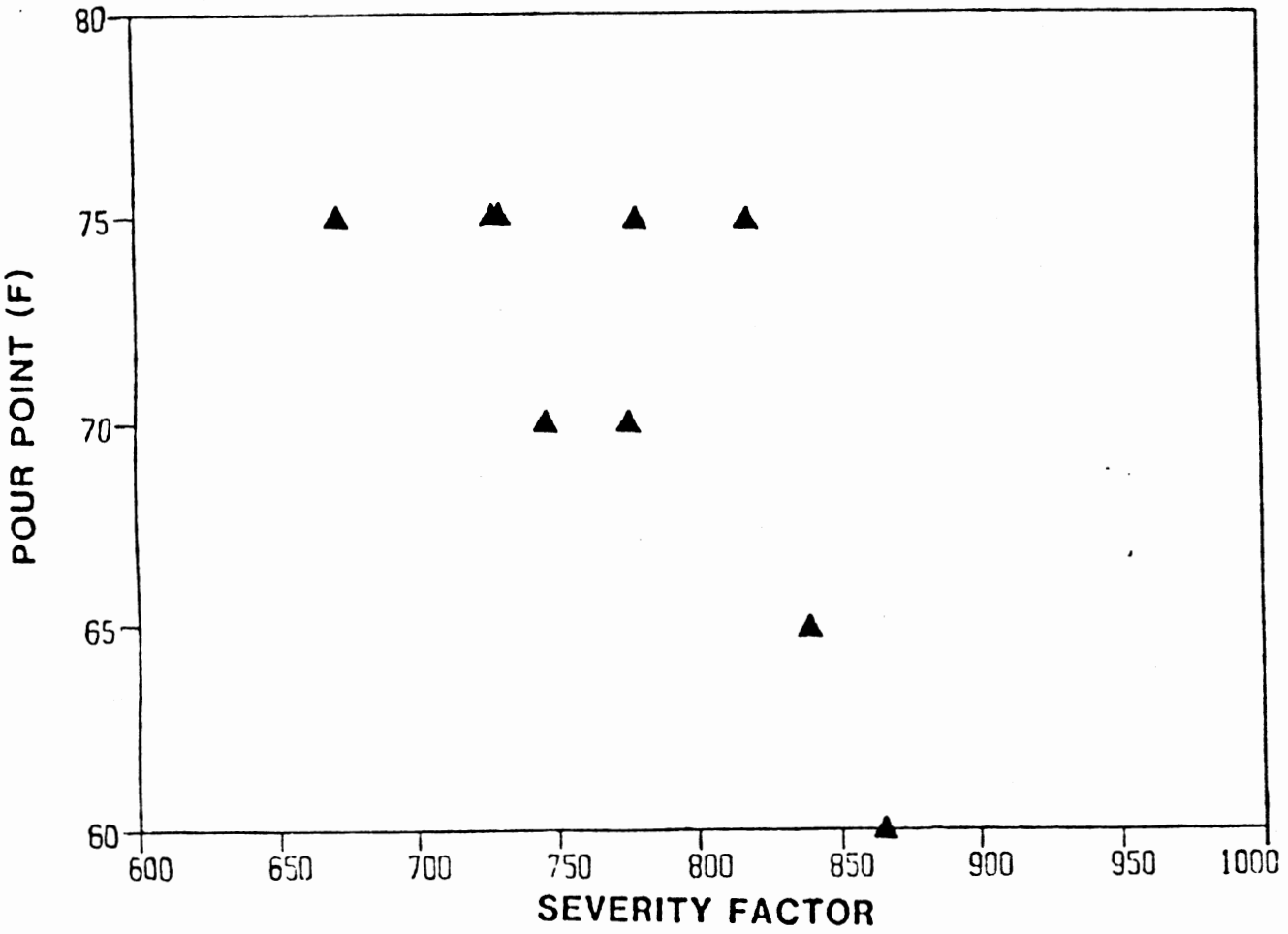

Figure 22. Pour Point Reduction as a Function of Linden and Reid's Severity Factor - Crude A

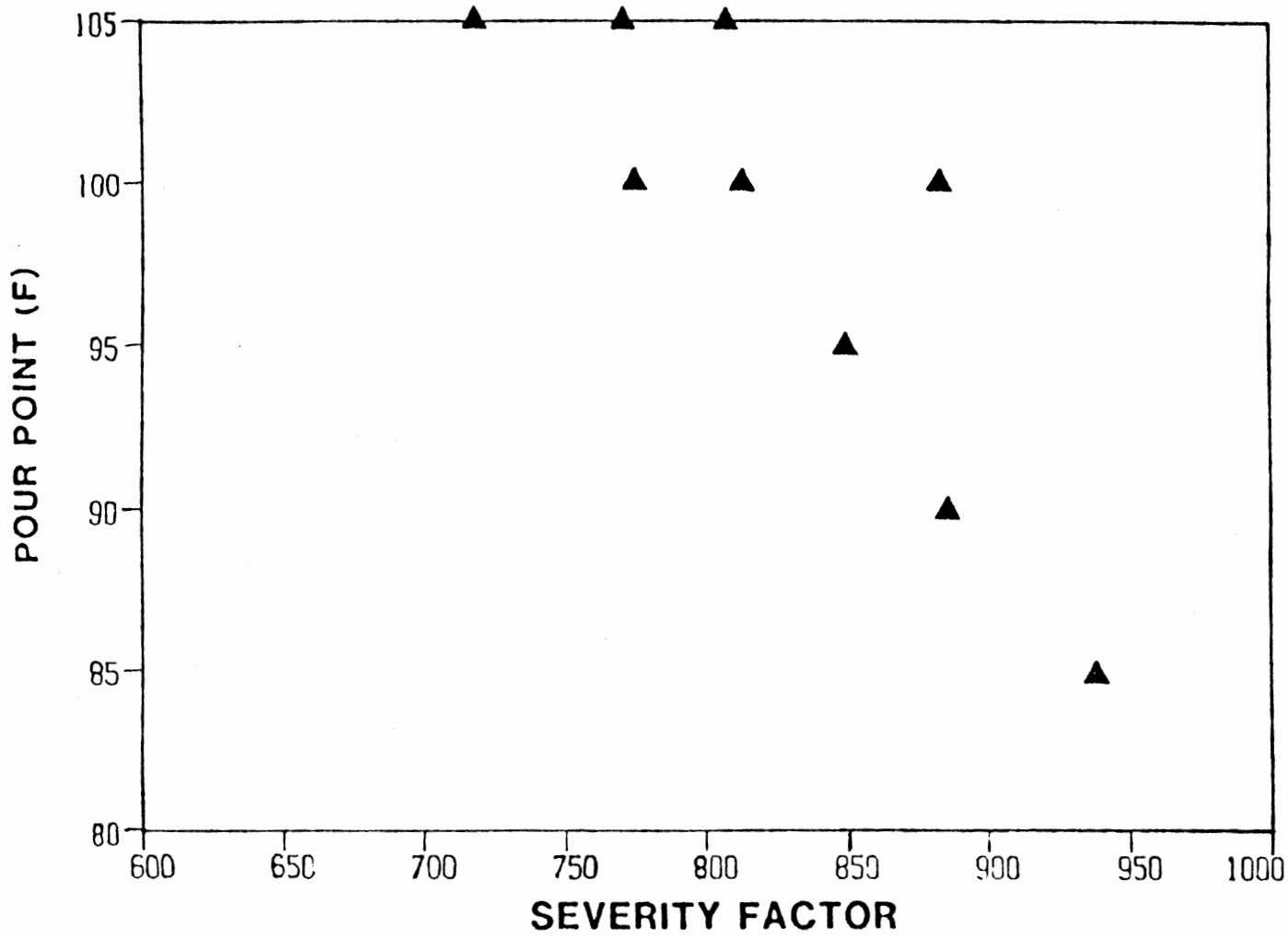

Figure 23. Pour Point Reduction as a Function of Linden and Reid's Severity Factor - Crude B

APPENDIX E

EQUIVALENT REACTOR VOLUME CALCULATIONS

For determining the space time of the crude in the reactor one must first calculate the equivalent reactor volume V_R:

$$V_R = \frac{1}{\exp\left(\frac{-E}{RT_R}\right)} \int_o^V \exp\left(\frac{-E}{RT}\right) dV$$

or

$$V_R + \frac{A}{\exp\left(\frac{-E}{RT_R}\right)} \int_o^x \exp\left(\frac{-E}{RT}\right) dx$$

To evaluate the integral, a plot of temperature versus length must be obtained. A typical profile is given in Figure 12 (400°C). Next -E/RT must be calculated as a function of L. Plotting $e^{-E/RT}$ versus L and determining the area under the curve enables one to calculate the value of the integral. The following calculations were done and are shown here for ease to the reader.

CRUDE A T = 400°C

$A_{reactor} = .0253\ in^2$

$V_{reactor} = .3039\ in^3$

$T_r = 414°C$

$$\frac{-E}{RT_R} = \frac{-30000\ cal\ mole \cdot k}{mole\ 1.987\ cal\ (414 + 273) \cdot k} = -21.98$$

$$\exp^{-21.98} = 2.95 \times 10^{-10}$$

$$\frac{A}{\exp^{-E/RT_R}} = \frac{.0253\ in^2}{2.85 \times 10^{-10}} = 8.86 \times 10^7\ in^2$$

T (k)	-E/RT	$e^{-E/KT}$ ($x10^{-2}$)	L (in)
575	26.26	.0395	0
649	23.26	.7885	1
671	22.5	1.6906	2
678	22.27	2.13	3
687	21.98	2.86	4
687	21.98	2.86	5
687	21.98	2.86	6
687	21.98	2.86	7
687	21.98	2.86	8
687	21.98	2.86	9
687	21.98	2.86	10
687	21.98	2.86	11
687	21.98	2.86	12

Area under curve of $e^{-E/RT}$ vs L

2.89×10^{-9}

$V_R = (8.86 \times 10^7 \text{ in}^2)\ (2.89 \times 10^{9}) = .2561 \text{ in}^2$

$v_e \cdot \rho_e \cdot 1/\rho g = v_g$

at

$v_e = 3.93$ ml/min; $v_g = 1560.49$ ml/min

$v_e = 1.57$ ml/min; $v_g = 582.24$ ml/min

$v_e = .786$ ml/min; $v_g = 350.76$ ml/min

at 400°C, 20% of crude A is vaporized

$$(.8)(v_e) + .2)\ v_g = v$$

at

$v_e = 3.93$ ml/min; $v = 315.24$ ml/min

$v_e = 1.6$ ml/min; $v = 117.7$ ml/min

$v_e = .8$ ml/min; $v = 70.78$ ml/min

$$\tau = \frac{V}{v}$$

at

$v_e = 3.9$ ml/min; $\tau = .80$ sec

$v_e = 1.6$ ml/min; $\tau = 2.14$ sec

$v_e = .8$ ml/min; $\tau = 3.56$ sec

CRUDE A T = 500°C

T_R = 529°C

$$\frac{-E}{RT_R} = \frac{-30000}{1.987\ (529 + 273)} = -18.83$$

$$e^{-18.83} = 6.67 \times 10^{-9}$$

$$\frac{A}{e^{-E/RT_R}} = 3.79 \times 10^{6}\ in^2$$

T (k)	-E/RT	$e^{-E/KT}$ (x10^{-2})	L (in)
573	26.35	.004	0
723	20.88	.853	1
743	20.32	1.496	2
771	19.58	3.13	3
778	19.41	3.73	4
783	19.28	4.22	5
802	18.82	6.67	6
802	18.82	6.67	7
802	18.82	6.67	8
802	18.82	6.67	9
802	18.82	6.67	10
802	18.82	6.67	11
802	18.82	6.67	12

Area under $e^{-E/RT}$ vs L diagram = 57 x 10^{-9}

$V_R = (3.793 \times 10^6)(57 \times 10^{-9}) = .2162\ in^2$

at 500°C 37.5% Crude A is vaporized

at

$v_e = 3.9$ ml/min; $\tau = .27$ sec

$v_e = 1.6$ ml/min; $\tau = .67$ sec

$v_e = .8$ ml/min; $\tau = 1.51$ sec

CRUDE A T = 500°C

T_R = 629°C

$$\frac{-E}{RT_R} = -16.73$$

$$e^{-E/RT_R} = 5.377 \times 10^{-8}$$

$$\frac{A}{e^{-E/RT_R}} = 4.71 \times 10^{5}$$

T (k)	-E/RT	$e^{-E/KT}$ ($\times 10^{-2}$)	L (in)
573	26.35	.004	0
753	20.05	1.96	1
777	19.43	3.64	2
829	18.21	12.32	3
864	17.47	25.76	4
876	17.24	32.72	5
903	16.72	54.79	6
903	16.72	54.79	7
903	16.72	54.79	8
902	16.72	53.78	9
902	16.74	53.78	10
902	16.74	53.78	11
902	16.74	53.78	12

Area under curve $e^{-E/RT}$ vs L diagram = 4.28×10^{-7}

$V_R = (4.705 \times 10^5)(4.28 \times 10^{-7}) = .2014 \text{ in}^2$

at 600°C .55% Crude A is vaporized

at

$v_e = 3.9$ ml/min; $\tau = .15$ sec

$v_e = 1.6$ ml/min; $\tau = .44$ sec

$v_e = .8$ ml/min; $\tau = .79$ sec

VITA

Diana Bray Fenton

Candidate for Degree of

Master of Science

Thesis: POUR POINT REDUCTION OF HEAVY CRUDE OILS BY THERMAL TREATMENT

Major Field: Chemical Engineering

Biographical

Personal Data: Born in Ponca City, Oklahoma, September 1, 1961 the daughter of Bruce G. and Emma R. Bray. Married to Jeff T. Fenton on May 21, 1983.

Education: Graduated from Ponca City High School, Ponca City, Oklahoma, in May, 1979; received Bachelor of Science Degree in Chemical Engineering from Oklahoma State University in May, 1983; completed requirements for the Master of Science degree at Oklahoma State University in May, 1987.

Professional Experience: Laboratory researcher at Conoco, Inc., Ponca City, Oklahoma, May to August, 1981; Teaching Assistant, Department of Chemical Engineering, Oklahoma State University, August, 1983 to December, 1984, Employed as an Engineer at Vista Chemical Company, Ponca City, Oklahoma, May, 1985 to present.